# Pyrazolylborate Cyanometalate Single-Molecule Magnets

Philip J. Ferko<sup>1</sup> and Stephen M. Holmes<sup>1,2,\*</sup>

**Abstract:** This review summarizes recent developments in the field of single-molecule magnets derived from paramagnetic cyanometalate complexes supported by pyrazolylborate ancillary ligands. This review describes developments between 2002 and 2013 and is restricted to descriptions of molecular cyanometalate precursor complexes, their magnetic polynuclear single-molecule magnet derivatives, and common structural archetypes.

**Keyword:** Cyanometalates, magnetic, polynuclear complexes, single-molecule magnet.

#### 1. INTRODUCTION

Considerable attention has been paid to the development of superparamagnetic complexes, known collectively as single-molecule magnets (SMMs), as they represent an interesting and intensely studied class of magnetic materials that can be easily prepared, tuned, and can studied via a range of spectroscopic and magnetic characterization techniques [1-9]. The most celebrated class of SMMs are those containing transition metal centers linked via oxo- and carboxylate bridges, with  $\{Mn_{12}O_{12}(O_2CMe)_{16}(OH_2)_4\}$  receiving the most attention. In these soluble, molecular, single domain clusters a large spin ground state ( $S_T = 10$ ) is found due to efficient antiferromagentic interactions between the Mn<sup>IV</sup> (S =  $^{3}/_{2}$ ) and Mn<sup>III</sup> (S = 2) spin centers. A nearly parallel alignment of its Jahn-Teller axes at the MnIII sites leads to uniaxial Ising-like magnetic anisotropy (where D < 0 with small E for the Hamiltonian:  $H = DS_{T,z}^{2}$ ) and superparamagnetic-like magnetic relaxation is seen. Under ideal circumstances these and other anisotropic complexes exhibit sizable energy barriers to magnetization reversal, where  $\Delta$  ~  $|D|S_T^2$  or  $\Delta = |D|(S_T^2 - \frac{1}{4})$  for integer or half-integer  $S_T$  values, respectively [1-12].

In SMMs the creation of an energy barrier ( $\Delta$ ) between two thermodynamically equivalent  $m_S = \pm S$  configurations allows for the observation and monitoring of slow relaxation dynamics using a variety of magnetization measurements [7-12]. Below  $T_B$ , the so-called "blocking temperature", the available thermal energy is insufficient to overcome  $\Delta$  and the spin becomes trapped in one of two possible spin configurations. Application of large external magnetic fields (H) saturate the magnetization (M) of the sample and upon removal of this DC field ( $H_{dc} = 0$ ), M slowly decays towards zero with a characteristic relaxation time ( $\tau$ ). The relaxation time usually exhibits thermally activated behavior and can be measured by following changes in magnetization (M) as a function of time or the frequency ( $\nu$ ) dependence of the AC

susceptibility. At very low temperatures, quantum tunneling of the magnetization (QTM) is often seen- this is relaxation of the magnetization at a faster rate than thermally activated pathways allow [7-13]. With sufficiently large spin reversal energy barriers slow magnetization relaxation can be observed at low temperatures. To our knowledge  $[Mn^{III}_{6}O_{2}(Et-sao)_{6}(O_{2}CPhMe_{2})_{2}(EtOH)_{6}]$  displays the highest spin reversal barrier ( $\Delta = 86$  K) for this SMM class [9].

Over the past twenty years several successful synthetic strategies have been developed for the preparation of polynuclear complexes with higher spin ground states. The majority of oxo- and carboxylate SMMs contain first-row transition metal ions and generally exhibit small zero-field splitting terms ( $D \sim -0.1-0.2 \text{ cm}^{-1}$ ) because orbital angular momentum contributions to their magnetic ground states are effectively quenched by the low symmetry environment of the 3d ions [6-8, 10-13]. As a general trend, when the overall spin ground state of polynuclear complexes increases, the uniaxial magnetic anisotropy |D| becomes proportional to  $S_T$ thus leading to lower SMM energy barriers which generally scale as a function of  $S_T^{o}$  rather than  $S_T^{2}$  [14, 15]. Unfortunately, while many analogues with exceptionally high spin ground states are known,  $\Delta$  is often lower than expected due to insufficient magnetic anisotropy control and rapid QTM.

In an effort to better tune magnetic bistability, worldwide attention has naturally turned towards the selective introduction of metal centers with orbital contributions to their spin ground states. A variety of synthetic strategies have been explored by incorporating transition metals with even greater single-ion anisotropy, either via spin state (large zero-field splitting parameters, D) or introduction of orbital anisotropy (large spin-orbit parameter,  $\lambda$ ), into various polynuclear complexes. In polynuclear complexes control of the single-ion anisotropy tensors has received particular attention in an attempt to influence the zero-field splitting term of the Hamiltonian. Efforts include the use of sterically demanding polydenate ligands to preferentially orient the relative orientations of Jahn-Teller axes and/or single-ion anisotropy tensor orientations during the self-assembly process [6, 8, 11].

<sup>&</sup>lt;sup>1</sup>Department of Chemistry and Biochemistry, University of Missouri-St. Louis, St. Louis, MO 63121, USA

<sup>&</sup>lt;sup>2</sup>Center for Nanoscience, University of Missouri-St. Louis, St. Louis, MO 63121, USA

<sup>\*</sup>Address correspondence to this author at the Department of Chemistry and Biochemistry, University of Missouri-St. Louis, St. Louis, MO 63121, USA; Tel: +01-314-516-4382; Fax: +01-314-516-5342; E-mail: holmesst@umsl.edu

Some of these synthetic approaches exploit heavy metal ions as a route for systematically introducing centers with large orbital contributions to their magnetic ground states. As spin-orbit coupling is a relativistic effect, various SMMs containing paramagnetic *f*-elements [16-39] have been investigated, as their orbital contributions are significant and unquenched by the ligand field under ideal circumstances. Insertion of lanthanides [20-32] and actinides [33-39] into various polynuclear complexes can lead to degenerate spin round states and afford so-called hybrid d-f compounds [16-32]- in some cases higher spin reversal energy barriers are observed but systematic control of their single-ion tensors remains a difficult issue of practical importance.

As a logical extension of this approach, reducing the numbers of paramagnetic ions to a few or single metal center, gives a series of molecules that also exhibit slow dynamics. The smallest members of the f element series have  $[LnPc_2]^n$  stoichiometry, where Ln = Tb, Dy, Ho (for  $n = \pm 1$ , 0) [20, 25, 28, 32]. A complimentary approach where "smaller is better" concerns structurally related mononuclear 2- and 4-coordinate 3d complexes [40-48]. Many of these display frequency-dependent behavior [40, 42-44, 46, 54, 55] owing to unquenched orbital angular momentum and well-isolated  $m_1$  states that ultimately lead to comparatively high thermal barriers to magnetization reversal [up to  $\Delta =$ 325(4) K]; surprisingly slow dynamics can be observed below ca. 29 K in a two-coordinate and linear Fe<sup>1</sup> complex [50]. In these mononuclear iron complexes, spin-orbit interactions give rise to significant magnetic anisotropy, in addition to efficient coupling to lattice phonon modes, via vibronic interactions (e.g. Renner-Teller effect); in such cases rapid QTM under an applied static magnetic field [50] was seen. As a general statement an experimentalist must (1) maximize magnetic anisotropy and (2) minimize the extent that dipolar interactions contribute to rapid magnetic relaxation when attempting to control the magnetic properties of SMMs. This review will discuss world-wide efforts to address both criteria in cyanometalate-based SMMs containing sterically demanding tripodal pyrazolylborate ligands.

#### LIST OF ABBREVIATIONS

Tp hydridotris(pyrazolyl)borate

Tp\* hydridotris(3,5-dimethylpyrazol-1-yl)borate

 $\mathsf{Tp}^{\mathsf{Me},\mathsf{me}3}$ hydridotris(3-methyl-4,5-propylene-5-

methylpyrazol-1-yl)borate

 $T\mathfrak{p}^{Me,mt4}$ hydridotris(3-methyl-4,5,6,7-

tetrahydroindazolyl)borate

 $\mathsf{Tp}^{\mathsf{Ph}}$ hydridotris(pyrazolyl)phenylborate

MeTp methyltris(pyrazolyl)borate

iBuTp 2-methylpropyltris(pyrazolyl)borate

tetrakis(pyrazolyl)borate pzTp

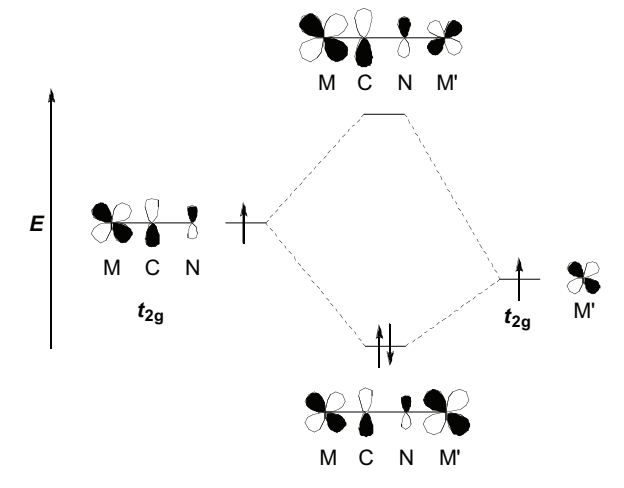
 $\text{Tp}^{4\text{Bo}}$ hydridotris(indazolyl)borate

 $T\mathfrak{p}^{\mathbf{*}^{Bn}}$ hydridotris(3,5-dimethyl-4-

benzyl)pyrazolylborate

tacn 1,4,7-triazacyaclononanes

### Antiferromagnetic Exchange



### Ferromagnetic Exchange

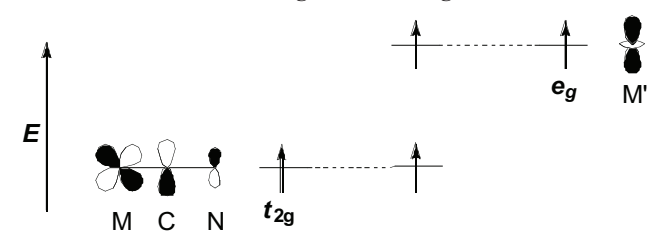


Fig. (1). Idealized cyanide-mediated superexchange interactions between octahedral paramagnetic ions.

N,N',N''-trimethyl-1,4,7-triazacyclononane Me<sub>3</sub>tacn

 $\mathrm{Tp}^{4\mathrm{Bo}}$ hydridotris(indazolyl)borate

dpa 2,2'-dipyridylamine

triaminocyclohexane tach

triphos 1,1,1-tris(diphenylphosphanylmethyl)ethane

2,6-bis(benzimidazol-2-yl)pyridine bmpy

bpy 2,2'-bipyridine

4,4,5,5-tetramethylimidazoline-1-oxyl-2-(2'-IM-2Py

pyridyl)

cyclen 1,4,7,10-tetraazacyclododecane

# 2. MAGNETIC CYANOMETALATES

Cyanometalates are excellent building blocks for constructing molecule-based polynuclear complexes because cyanides generally form linear M(µ-CN)M' linkages, stabilize a variety of transition metal centers and oxidation states, and efficiently communicate spin density information [59-69]. Furthermore, the sign and magnitude of the local exchange interactions can be controlled via substitution and often predicted using simple orbital symmetry arguments (Fig. 1) [59-64, 68]. Under ideal circumstances these molecular precursors will self assemble towards a common structural archetype, and by systematic variation of ligands and metal centers present, afford a family of polynuclear derivatives whose properties are derived from their component building blocks.

Scheme 1. Dimensional reduction of an idealized Prussian blue structure into discrete polynuclear complexes.

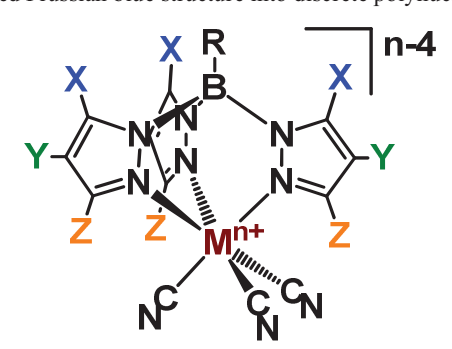


Fig. (2). Idealized structure of [(Tp<sup>R</sup>)M<sup>n</sup>(CN)<sub>3</sub>]<sup>n-4</sup> building blocks.

The primary advantages for investigating polynuclear cyano complexes are that the synthetic chemistry is generally straightforward, the magnetic interactions are often simple to predict and rationalize, and the exchange interactions do not exhibit dramatic structure-dependent changes in sign like  $M(\mu-O)M'$  units in oxo/carboxylate SMMs [4]. For example, assuming that octahedral metal ions are present and that they are linked via a shared cyanide bridge, Goodenough-Kanamori [64, 68] rules stipulate that ferromagnetic interactions will occur when unpaired electrons reside in orthogonal orbitals [e.g.  $\text{Fe}^{\text{III}}_{\text{LS}}(t_{2g})$  and  $\text{Ni}^{\text{II}}(e_g)$ ; Fig. (1), bottom] while antiferromagnetic ones [Fig. (1), top] will dominate when they have the same symmetry [59-64]. However, an important caveat is that the typical exchange parameter in cyanidebased systems is generally smaller (e.g.  $J \sim 5-50 \text{ cm}^{-1}$ ) than those encountered for oxo- or radical-bridged metal centers [4, 21, 22, 70], and this often leads to small values of  $\Delta$ .

Three important factors appear necessary for establishing magnetic anisotropy and an energy barrier to spin reversal in cyanide-based SMMs: (1) they must contain paramagnetic metal centers with substantial first-order orbital angular momentum contributions, (2) possess a degenerate spin ground state, and (3) be well-separated in the solid state [10-13, 71-73]. In these cyanide-based SMMs the total angular momentum projection ( $|M_J|$ ) appears to be a critical factor for establishing negative cluster anisotropy and an activation energy barrier ( $\Delta$ ) to thermal magnetization reversal. In contrast, many early 3d oxide-bridged clusters [e.g.  $Mn_{12}O_{12}(OAc)_{16}(OH_2)_4$ ] are considered as spin systems where orbitally nondegenerate metal centers exhibit weak single-ion and second-order anisotropy, whose barrier

heights  $(\Delta \sim S^2|D|)$  are to a first approximation, directly proportional to the product of the spin ground state squared  $(S^2)$  and zero-field splitting parameter (D) [10-13,71-73]. Under ideal circumstances efficient spin coupling and magnetic anisotropy give polynuclear cyanide-based complexes that exhibit slow relaxation of the magnetization despite their comparatively small spin ground states.

#### 3. ANCILLARY LIGAND ROLE

Polynuclear cyanide-based SMMs are often constructed via the self-assembly of various paramagnetic precursors or building-blocks that exhibit substantial (first-order) orbital angular momentum contributions to their spin ground states [10-13, 71-74]. Using the concept of dimensional reduction [Scheme 1] the geometric arrangement and numbers of cyanides available for bridging to adjacent metal centers may be controlled via proper choice of ancillary ligand. Polydentate ligands are commonly used in the construction of multinuclear SMMs, as they rigorously enforce the chosen coordination geometry, while simultaneously tuning the steric, electronic, and redox properties of the complex. The most commonly used building-blocks, or cyanometalate complexes used to construct polynuclear derivatives, are those derived from [fac-LM(CN)<sub>3</sub>]<sup>n</sup>-ions, where L is a series of tridentate ligands (Fig. 2) [10, 13, 71, 74-79].

While numerous cyano complexes contain tridentate *fac*-and *mer*-coordinate ligands the most versatile ones used in the construction of discrete molecular SMMs are those incorporating pyrazolylborates (Tp<sup>R</sup>). Of these, complexes of generalized [(Tp<sup>R</sup>)M(CN)<sub>3</sub>]<sup>n</sup> stoichiometry find the greatest

Fig. (3). Commonly used pyrazolylborate ligands in construction of various cyanometalate-based single-molecule magnets.

utility in the preparation of polynuclear derivatives due to a number of factors:

- (1) Poly(pyrazolyl)borate ligands (Tp<sup>R</sup>) are easily prepared and modified at each of their ten substitutable positions (Fig. 3) [80-96]. Installation of various functional groups allows for atom-economical tuning of their electronic states, solubility, and steric requirements.
- (2) Poly(pyrazolyl)borates (Fig. 3) stabilize multiple oxidation states for most transition metal centers and enables a series of structurally related building blocks to be constructed. The overall charge, numbers of unpaired electrons, energies, and orbital degeneracies may be systematically controlled upon insertion of various transition metal centers [80-103].
- (3) Surprisingly few paramagnetic [fac-LM<sup>II</sup>(CN)<sub>2</sub>] and [fac-LM<sup>II-IV</sup>(CN)<sub>3</sub>] complexes are known and low-valent early metal derivatives are rare. In addition to pyrazolylborates, Me<sub>3</sub>tacn [10,75,104-112], tacn [10, 75, 104, 107, 108, 148], tach [113], and triphos [71, 76, 78, 79, 114-116], and cyclopentadienyl (Cp and Cp\*) [117-121] also see extensive use. Pyrazolylborates stabilize a number of low-valent centers (e.g. V<sup>II,III</sup>, [99]; Ti<sup>III</sup>, [103]; Cr<sup>II</sup>, [102]; Mn<sup>II,III</sup>, [100, 101]; Nb<sup>III</sup>, [103]).

Several reports indicate that the steric demand of ancillary ligands and reaction stoichiometry can be exploited to direct the self-assembly of building blocks toward a common structural archetype [10, 11, 13, 97, 98, 122-127]. During self-assembly of molecular components, the steric demand of the building blocks and the spatial orientations of formed cyanide bridges are intimately involved in creating polynuclear complexes whose magnetic anisotropy tensor orientations may be systematically controlled at the molecular level. Under ideal circumstances complexes with sufficiently high SMM energy barriers to observe slow magnetic relaxation dynamics may be isolated [13, 77, 98-101, 104-154].

Using this simple synthetic strategy the concept of molecular symmetry and its influence on magnetic anisotropy has been explored by several groups [12, 77, 98, 109, 110, 125, 126, 135, 139]. For example, Zuo and coworkers indicate that the SMM barrier is enhanced upon conversion of cubic  $\{Fe^{III}_{6}Cu^{II}_{8}\}$  ( $\Delta/k_{B} = 11.3$  K) to a trigonal bipyramidal  $\{Fe^{III}_{2}Cu^{II}_{3}\}$  complex ( $\Delta/k_{B} = 23.2$  K) (Figs. **4a** and **4b**] [10, 77, 109-111, 131]. In later work, Zhang et al. also demonstrated that magnetic anisotropy and thermal SMM energy barriers in {Fe<sup>III</sup><sub>4</sub>Ni<sup>II</sup><sub>4</sub>} complexes [see section 5.6, Fig. 15] were changed upon symmetry reduction [125, 135]. The authors demonstrated that single-ion anisotropy tensor alignment, rather than molecular symmetry, is the most important factor in establishing an SMM barrier. In this study the magnetic properties of cubic symmetry {Fe<sup>III</sup><sub>4</sub>Ni<sup>II</sup><sub>4</sub>} molecular boxes were compared to those lower symmetry  $(C_2)$ . The magnetic data indicated that the exchange couplings were identical and the large differences in zero-field and  $\Delta$  parameters were ascribed to the relative orientations of their putative single-ion anisotropy tensors ( $Fe^{III} \cdots B$  axes) at the [ $(Tp^R)Fe^{III}(CN)_3$ ] sites. While reduction of cluster symmetry does occur via insertion of sterically demanding Tp<sup>R</sup> ligands, the parallel orientation of the  $C_3$  axes in the  $C_2$ -symmetric complex appears to be directly related to the formation of a higher SMM barrier ( $\Delta/k_{\rm B} = 33$  K) [135].

While a significant number of cyanide-based SMMs have been described over the past decade an overarching strategy for tuning the magnitude of their spin reversal barriers has remained elusive. In these complexes it appears that the single-ion tensor orientations play a critical but poorly understood role in creating an energy barrier to spin reversal and significant resources and efforts have been expended towards the realization of this goal. In the following sections various attempts to systematically engineer polynuclear complexes with using a variety of molecular building blocks are described.

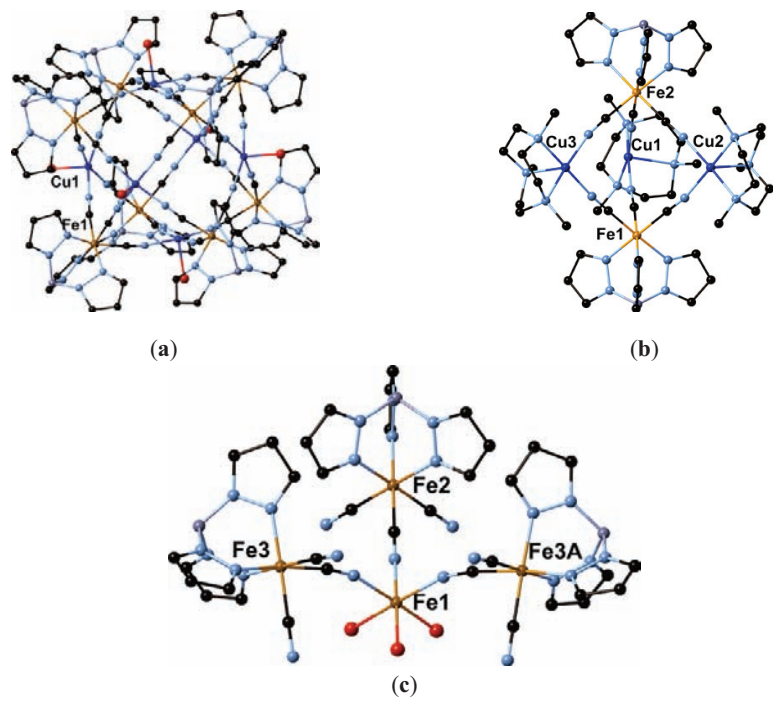


**Fig. (4).** X-ray structures for early Tp-based polynuclear complexes: (a) {Fe<sup>III</sup><sub>8</sub>Cu<sup>II</sup><sub>6</sub>}, (b) {Fe<sup>III</sup><sub>2</sub>Cu<sup>II</sup><sub>3</sub>}, and (c) {Fe<sup>III</sup><sub>4</sub>}. Those depicted in a and b are SMMs [77, 109, 97].

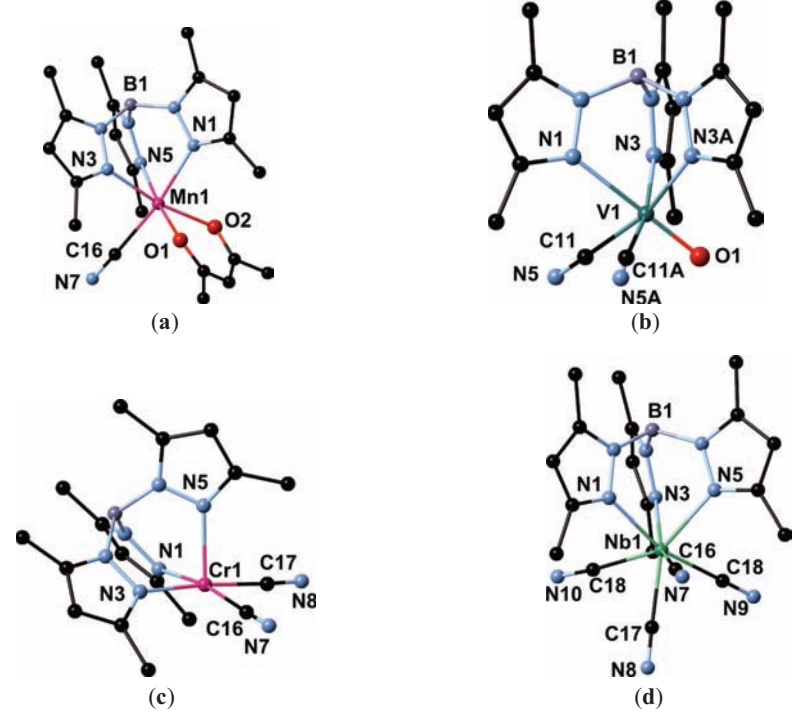


**Fig. (5).** X-ray structures of various cyanometalate complexes: (a)  $[NEt_4][(Tp^*)Mn^{II}(acac)(CN)][100,101]$ , (b)  $[NEt_4][(Tp^*)M^{IV}O(CN)_2](M^{IV} = Ti, V)[99, 103]$ , (c)  $[NEt_4]_2[(Tp^*)Nb^{III}(CN)_4](M^{II} = Cr, Co, Ni)[102]$ , and (d)  $[NEt_4]_2[(Tp^*)Nb^{III}(CN)_4][103]$ .

### 4. BUILDING BLOCK PREPARATION

# 4.1. General Preparation

A variety of mono- [101], di- [99, 102], tri- [13, 98, 99, 103, 123, 124, 148, 150], and tetracyanometalate [103] complexes are prepared *via* two general synthetic methods. The most common approach affords cyanometalate salts in high yields *via* metathesis of known pyrazolylborate halo com-

plexes with excess tetra(alkyl)ammonium cyanide [13, 97, 103, 125, 132,135]. Most are six-coordinate complexes, while fewer numbers of five- and seven coordinate analogues are known (Figs. 5 and 6). A second approach, being limited to iron analogues, involves peroxide oxidation of  $(Tp^R)_2Fe^{II}$  followed by cyanide addition to give  $[cat][(Tp^R)Fe^{III}(CN)_3]$ , where  $[cat] = NEt_4^+$ ,  $NBu_4^+$ , and  $PPh_4^+$ . Alternatively, stepwise treatment of the chosen pyra-

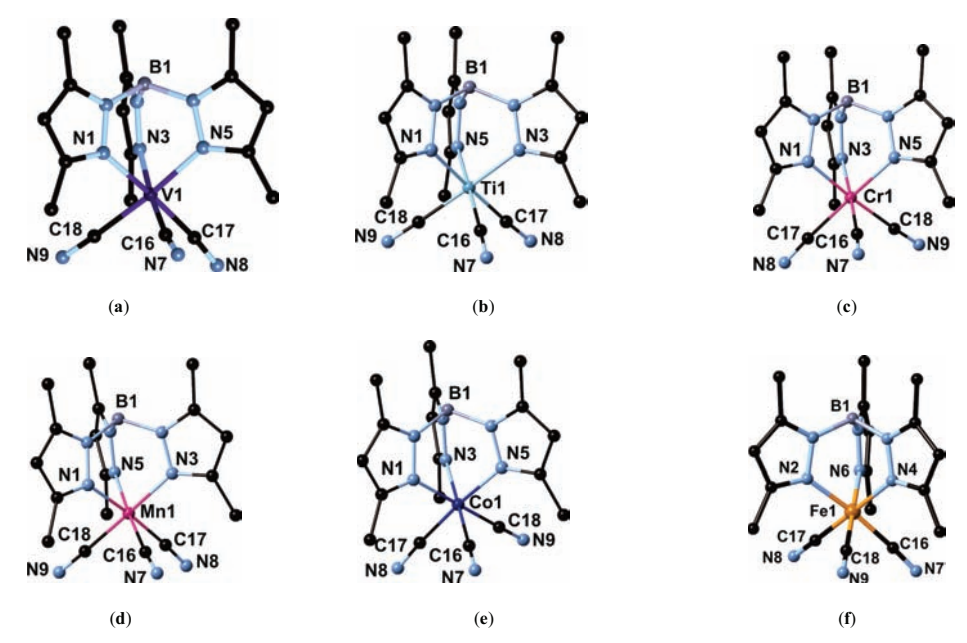


Fig. (6). X-ray structures of various 3d tricyanometalates: (a)  $[NEt_4]_2[(Tp^*)V^{II}(CN)_3]$  [99] and (b-f)  $[NEt_4]_2[(Tp^*)M^{III}(CN)_3]$  complexes  $[M^{III}(Tp^*)M^$ = Ti and Cr, [103]; Mn, [100, 101]; Co, [103]; Fe, [98, 123]).

zolylborate salt with iron(III) chloride or [Fe<sup>III</sup>OCl<sub>6</sub>]<sup>2-</sup>, followed by excess cyanide affords the desired tricyano complex [135]. Representative examples of these mononuclear cyanometalates, their structures (Figs. 5 and 6), and magnetic properties (Table 1) are described in subsequent sec-

#### 4.2. Mono- and Dicyanometalates

Mono- and dicyanometalate complexes are known to contain a variety of five- and six-coordinate metal centers. A magnetically isotropic  $S = \frac{5}{2}$  monocyano complex of [NEt<sub>4</sub>][(Tp\*)Mn<sup>II</sup>(acac)CN] stoichiometry was prepared via the sequential treatment of manganese(III) acetylacetonate with KTp\* followed by [NEt<sub>4</sub>]CN, and isolated as airsensitive crystals (Fig. 5a) [100, 101]. Two six-coordinate oxo complexes of  $[NEt_4][(Tp^*)M^{IV}O(CN)_2][M^{IV} = Ti, V]$ stoichiometry are prepared via exposure of their corresponding trivalent tricyanides to air (Fig. 5b) [99, 103]. Consistent with their formal oxidation states they exhibit S = 0 and  $\frac{1}{2}$ spin ground states, respectively. Three five-coordinate dicyanometalate pyramidal complexes  $[NEt_4][(Tp^*)M^{II}(CN)_2]$  stoichiometry are also known  $(M^{II} =$ Cr, Co, Ni) and spin ground states of S = 2,  $\frac{1}{2}$ , and zero are found, respectively (Fig. 5c) [102]. Surprisingly, the orbital contributions are nearly quenched in these  $C_s$ -symmetric square pyramidal anions.

A possible explanation for why orbital contributions are largely absent in these ions was proposed for a series of structurally related 5-coordinate square pyramidal complexes (not containing Tp<sup>R</sup> ligands) by Murugesu et al. [145]. The authors proposed that changing the Co<sup>II</sup> ion distance relative to the basal plane has a profound effect on the experimentally determined values of g and D. They demonstrated that for small Co<sup>II</sup>...plane distances, the zero-field parameter is rather small and  $g \sim 2$ . However at longer distances, D rapidly becomes large and negative, and slow magnetic relaxation becomes evident in the AC susceptibility data [145]. This effect is likely related to changes in spin-orbit coupling associated with ligand-induced distortions of the crystal field, and is currently the subject of high-field EPR investigations. By analogy, the small CoII...basal plane distance, defined by two pyrazole nitrogen and cyanide carbon atoms in [(Tp\*)Co<sup>II</sup>(CN)<sub>2</sub>], may also lead to negligible orbital contributions to the  $S = \frac{1}{2}$  spin ground state [102].

# 4.3. Tricyanometalates

The first reported tricyanoferrate(III) complex, [(Tp)Fe<sup>III</sup>(CN)<sub>3</sub>], and its tetranuclear {Fe<sup>III</sup><sub>4</sub>} derivative were reported by Lescouëzec et al. in 2002 (Fig. 4c) [97]. Since then a variety of di- and trivalent six-coordinate complexes of [cat]<sub>4-n</sub>[(Tp<sup>R</sup>)M<sup>n</sup>(CN)<sub>3</sub>] stoichiometry have been described, where  $M^{II} = V$ ;  $M^{III} = Ti [103]$ , V [99], Cr [148, 150], Mn [100,101], Fe [13, 97-99, 123, 125, 133, 135, 147, 149], and Co [103] (Fig. 6). If one initially assumes that these six-coordinate complexes adopt spin ground states that are identical to octahedral symmetry  $[M^n(CN)_6]^{n-6}$  ones, then magnetically isotropic  ${}^4A_2$  ( $S = {}^3/_2$ ) spin ground states should be found for V<sup>II</sup> and Cr<sup>III</sup>, while potentially anisotropic  $S = {}^1/_2$  ( ${}^2T_{2g}$ ; Ti<sup>III</sup> and Fe<sup>III</sup><sub>LS</sub>) and S = 1 ( ${}^2T_{2g}$ ; V<sup>III</sup> and Mn<sup>III</sup><sub>LS</sub>) ones are expected for the remaining analogues; Co<sup>III</sup> analogues are diamagnetic (S = 0) as expected [66, 67]. However, the  $[(Tp^R)M^n(CN)_3]^{n-4}$  complexes are actually  $C_{3v}$  symmetric and their magnetic properties can be dramatically different than those of their higher symmetry counterparts (Fig. 7).

We note that symmetry plays an often underappreciated role in whether appreciable spin-orbit interactions are observed in transition metal complexes. For example, when comparing the magnetic properties of  $[(Tp*)Mn^{III}(CN)_3]$  (idealized  $C_{3v}$  symmetry) to  $[Mn^{III}(CN)_6]^{3-}$  ( $O_h$  symmetry), the former complex exhibits an isotropic ( ${}^3A_2$  state, g=2.09) spin ground state while the latter one is anisotropic ( ${}^{3}T_{1}$  state,

cmpd.	S	g	ref.
$[\mathrm{NEt}_4][(\mathrm{Tp}^*)\mathrm{Ti}^\mathrm{III}(\mathrm{CN})_3]$	1/2	1.9	103
$\{[\operatorname{NEt}_4]_2[(\operatorname{Tp*})V^{II}(\operatorname{CN})_3]\} \cdot 2\operatorname{MeCN}$	3/2	2.01	99
$[\mathrm{NEt_4}][(\mathrm{Tp*})\mathrm{V^{III}}(\mathrm{CN})_3]\cdot 2\mathrm{H_2O}$	1	1.76	99
$[\mathrm{NEt_4}][(\mathrm{Tp*})\mathrm{V^{IV}}(\mathrm{O})(\mathrm{CN})_2] \cdot 2\mathrm{H_2O}$	1/2	2.06	99
[NEt <sub>4</sub> ][(Tp*)Cr <sup>III</sup> (CN) <sub>2</sub> ]	3/2	1.77	102
$[\mathrm{NBu_4}][(\mathrm{Tp})\mathrm{Cr^{III}}(\mathrm{CN})_3]$	3/2	2.0	148,150
[NEt <sub>4</sub> ][(pzTp)Cr <sup>III</sup> (CN) <sub>3</sub> ]	3/2	2.0	103
[NEt <sub>4</sub> ][(Tp*)Mn <sup>II</sup> (acac)CN]	5/2	1.93	101
[NEt <sub>4</sub> ][(Tp*)Mn <sup>II</sup> (3-NC-acac)CN]	5/2	2.00	101
$[cat][(Tp*)Mn^{III}(CN)_3]; [cat] = PPN^+, NEt_4^+$	1	2.09	100,101
$[\mathrm{NEt}_4][(\mathrm{Tp*})\mathrm{Co}^\mathrm{II}(\mathrm{CN})_2]$	1/2	2.09	102
$[cat][(Tp)Fe^{III}(CN)_3]; [cat] = K, NEt_4, NBu_4, PPh_4$	1/2	2.8	13,97
$[\mathrm{NEt_4}][(\mathrm{Tp*})\mathrm{Fe^{III}}(\mathrm{CN})_3]\cdot\mathrm{H_2O}$	1/2	2.92	116
$[\mathrm{NEt_4}][(\mathrm{pzTp})\mathrm{Fe^{II}}(\mathrm{CN})_3]$	1/2	2.41	116
[NEt <sub>4</sub> ][(Tp <sup>Me</sup> )Fe <sup>III</sup> (CN) <sub>3</sub> ]·3H <sub>2</sub> O	1/2	2.70	103
$[NEt_4][(Tp^{*Me})Fe^{III}(CN)_3]$	1/2	2.19	127
$[\mathrm{NEt_4}][(\mathrm{Tp^{*Bn}})\mathrm{Fe^{III}}(\mathrm{CN})_3]$	1/2	2.35	139
[NEt <sub>4</sub> ][(pz°Tp <sup>Me</sup> )Fe <sup>III</sup> (CN) <sub>3</sub> ]	1/2	2.58	103

Table 1. Magnetic Data Summary for Selected Paramagnetic Di- and Tricyanometalate Complexes

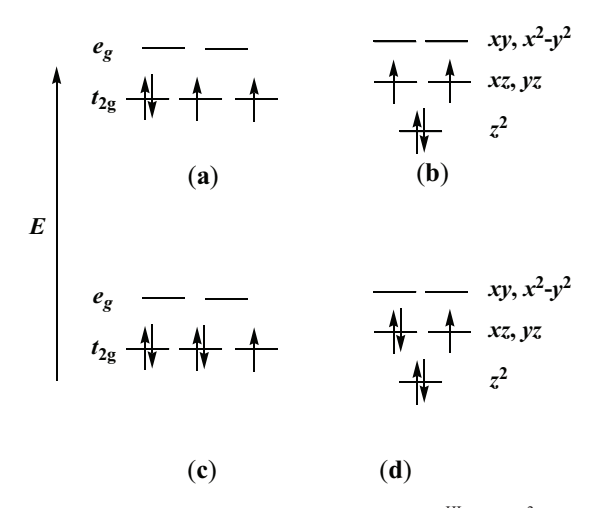


**Fig. (7).** Qualitative molecular orbital diagrams for magnetically anisotropic (a)  $[Mn^{III}(CN)_6]^{3-}$  and isotropic (b)  $[(Tp^*)Mn^{III}(CN)_3]^{-}$  anions. Qualitative molecular orbital diagrams for (c)  $Fe^{III}(CN)_6]^{3-}$  and (d)  $[(Tp^R)Fe^{III}(CN)_3]^{-}$  anions.

g = 2.39), owing to the presence of in-state first-order orbital contributions [66, 67, 100, 101] (Fig. 7).

To further investigate this assumption, the electronic configuration and spin ground state of the tricyanomanganate(III) complex was studied *via* Extended Hückel tightbinding (EHTB) calculations (Fig. 8) [101, 101]. The calculations show that the nearly degenerate d(xz) and d(yz) orbitals are found at slightly higher energies than the  $d(z^2)$  orbital (225 and 267 meV above, respectively); surprisingly, sig-

nificant  $\pi$ -type spin density is also delocalized into the Tp\* and cyanide ligands present [100, 101]. Therefore the electronic configuration of the two cyanomanganate(III) complexes, accounting for their symmetries are  $(z^2)^2(xz,xy)^2$  and  $(t_{2g})^4$  for  $[(Tp^*)Mn^{III}(CN)_3]^-$  and  $[Mn^{III}(CN)_6]^{3^-}$ , respectively (Figs. 7a and 7b]. Consequently the tricyano complex adopts an isotropic spin state (Fig. 7b) where the orbital contributions are nearly absent, while those for higher symmetry  $[Mn^{III}(CN)_6]^{3^-}$  are considerable [66, 67, 100, 101].

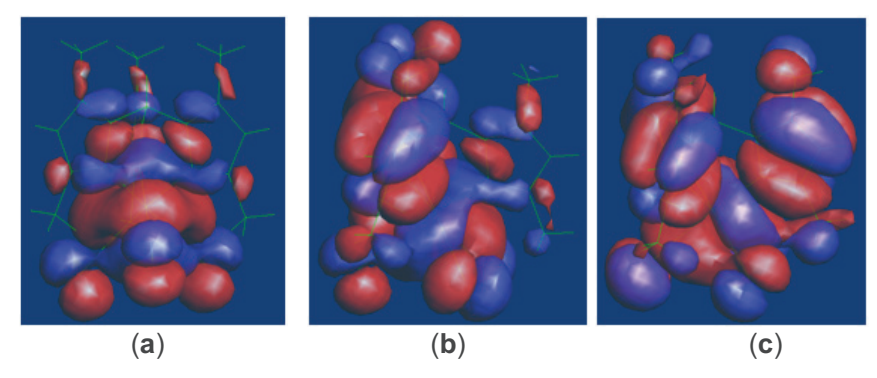


Fig. (8). Shapes of three lowest energy occupied orbitals in  $[NEt_4][(Tp^*)Mn^{III}(CN)_3]$  deduced from EHTB calculations: (a)  $d(z^2)$ , (b) d(xz), and (c) d(yz) orbitals. Figures taken from ref. 100. Copyright 2010 American Chemical Society.

Likewise, low-spin [(TpR)FeIILS(CN)3] complexes are also expected to have orbitally degenerate and thus magnetically anisotropic spin ground states (Figs. 7c). Under idealized  $C_{3v}$  symmetry, a  $(z^2)^2(xz,xy)^3$  electronic configuration gives a doubly degenerate  ${}^{2}E$  state and unquenched orbital angular momentum contributes to the  $S = \frac{1}{2}$  spin ground state [13, 66, 67, 77]. In comparison, the  $[Fe^{III}_{LS}(CN)_6]^3$  ion under  $O_h$  symmetry has an  $t_{2g}^5$  electronic configuration and gives an anisotropic  ${}^2T_{2g}$  spin ground state (g = 2.9) (Fig. 7d). Consequently, the Fe<sup>III</sup><sub>LS</sub> complexes display g-anisotropy, verifying that orbital degeneracy is necessary for generating considerable magnetic anisotropy [77, 98, 109, 110, 112, 131, 139, 141, 142, 143, 148]. Recent high-field EPR studies confirm that [(Tp<sup>R</sup>)Fe<sup>III</sup>(CN)<sub>3</sub>] complexes have spin ground states with significant g anisotropy;  $g_z$ ,  $g_y$ , and  $g_x$  values of 3.6, 2.2, and 2.0 were deduced for  $[NEt_4][(Tp^{*Me})Fe^{III}(CN)_3]$ [142]. The magnetic properties of several di- and tricyanometale complexes are summarized in Table 1.

Surprisingly, structural distortions also appear to play a poorly understood role in modulating magnetic anisotropy within a series of  $[(Tp^R)Fe^{III}_{Ls}(CN)_3]$   $(S = \frac{1}{2})$  anions and their polynuclear derivatives. Apparently, a qualitative relationship between the g parameter and Tp<sup>R</sup> induced distortions of the [fac-Fe<sup>III</sup>(CN<sub>3</sub>)] units may exist [12, 13, 77, 97, 98, 103, 110, 116, 118, 119, 125, 132, 133], where increasing steric demand of the tripodal ligand compress the Fe<sup>III</sup>(CN)<sub>3</sub> unit. As the C-Fe-C angle becomes more acute the g parameter generally increases and may indicate that structural distortions also influence the single-ion anisotropy properties of these tricyano complexes. This very issue is currently the focus of high-field EPR investigations [103, 132].

### 5. CYANIDE-BASED SINGLE-MOLECULE MAG-**NETS**

A basic requirement for constructing polynuclear SMMs are that anisotropic and paramagnetic transition metal centers be present and that adjacent metal centers participate in efficient magnetic exchange interactions. While oxo-carboxylatebased SMMs are well-known, cyanide-based polynuclear complexes that exhibit slow relaxation are fewer in numbers [10-13, 71-79, 98, 109-112, 122-129, 131-135, 137-144, 146, 152-154]. Over the past decade, a number of structurally related tricyanometalate-based SMM clusters, that despite their low spin ground states  $(1 \le S \le 6)$ , exhibit large D parameters

(up to -5 cm<sup>-1</sup>) and slow magnetic relaxation. Surprisingly only a few anisotropic metal centers (e.g. Fe<sup>III</sup>, [12, 13, 77, 97, 98, 109-112, 122-129, 131-135, 137-145, 147, 149]; Mn<sup>III</sup>, [71-73, 122]; Mo<sup>III</sup>, [10, 74, 75, 152]; Re<sup>II,IV</sup>, [10, 76, 79, 152, 154, 155]) have been exploited in the construction of these cyanide-based SMMs. However, most late transition metal analogues are not structurally related.

Of polynuclear complexes containing [(Tp<sup>R</sup>)M<sup>III</sup>(CN)<sub>x</sub>] building blocks only a few pyrazolylborate derivatives have been investigated (e.g.  $Tp^R = Tp$ , pzTp,  $Tp^*$ ). Those containing [(Tp<sup>R</sup>)M<sup>III</sup>(CN)<sub>3</sub>] units have garnered the greatest attention while dicyanometalate analogues are limited to tetranuclear squares, derived from paramagnetic  $[(Tp^*)V^{IV}O(CN)_2]^T$ and  $Mn^{II}$  ions [99]. Of polynuclear complexes derived from  $3d \left[ (Tp^R)M^n(CN)_z \right]^{(n-z-1)}$  (e.g.  $Tp^R = pzTp$ , Tp,  $Tp^*$ , etc.; z = pzTp2-3) building blocks those containing [(Tp<sup>R</sup>)Fe<sup>III</sup>(CN)<sub>3</sub>] anions generally exhibit slow relaxation of the magnetization above 1.8 K [77, 99-99, 109-112, 123, 125-129, 131-145, 147, 149]. In a typical synthesis treatment of these complexes with a variety of divalent salts affords several families of clusters, whose nuclearity and properties are strongly influenced by the steric demand of the pyrazolylborate and other ancillary ligands present. Under ideal circumstances these polynuclear complexes exhibit significant magnetic aniostropies arising from orbital contributions to their magnetic spin ground states [see section 4.3].

Insertion of paramagnetic ions into various SMMs structures can lead to magnetic anisotropy in their polynuclear derivatives assuming that the paramagnetic centers engage in efficient magnetic exchange interactions. A general structural feature of these SMMs is that the magnetically coupled metal ions are effectively shrouded by sterically demanding and close-packed ancillary ligands, which are generally inefficient conduits for spin density delocalization. As the majority of these complexes are also charged species, they tend to be well-separated in the solid state by charge balancing counterions and lattice solvent, further limiting intermolecular magnetic interactions. It follows that their magnetic properties are highly dependent on a variety of factors such as structure, symmetry, and intermolecular interactions.

### 5.1. Early Single-Molecule Magnets

Most cyanide-based single-molecule magnets contain octahedral  $[M^n(CN)_6]^{n-6}$  or  $C_{3v}$ -symmetric ions. The first

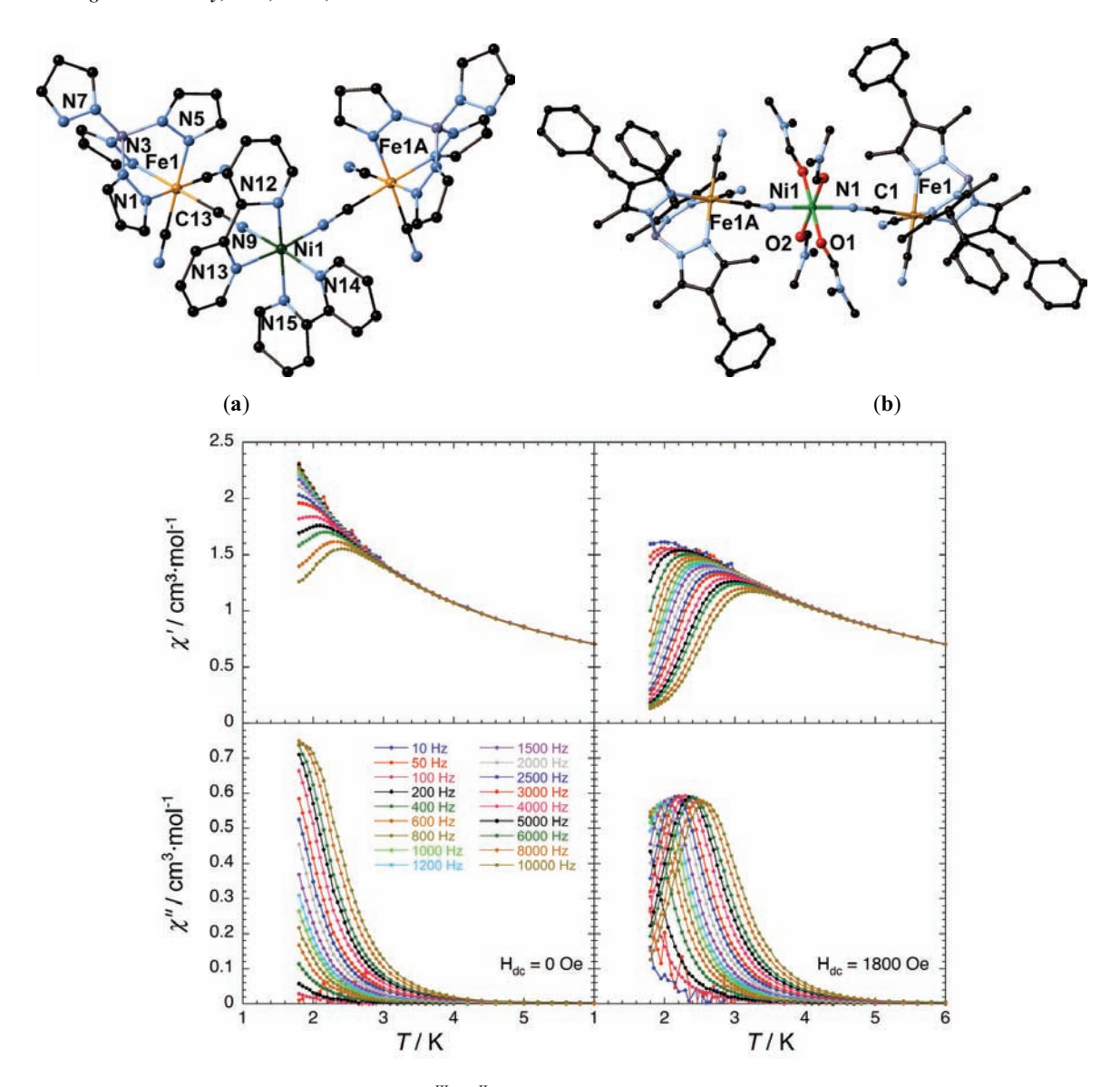


Fig. (9). (a and b) X-ray structures of two trinuclear  $\{Fe^{III}_2Ni^{II}\}\$  SMMs. In-phase ( $\chi'$ ) and out-of-phase ( $\chi''$ ) component of the AC susceptibilities for b for  $H_{dc}=0$  (bottom, left) and 1800 Oe (bottom, right). Figures taken from refs. [126] and [139]. Copyright 2010 Royal Society of Chemistry [126] and 2011 American Chemical Society [139].

cyanide-based SMM containing a pyrazolylborate ligand was reported by Zuo in 2004 [77]. The tetradecanuclear  $\{Fe^{III}_8Cu^{II}_6\}$  complex (Fig. 4a) contains an 8:6 ratio of cyanide-bridged  $C_{3v}$ -symmetric  $[(Tp)Fe^{III}(CN)_3]^T$  and  $[Cu^{II}-(OH_2)]^{2+}$  units, where the iron and copper centers reside at the corners and faces of an idealized cube, respectively [77]. Magnetic measurements show that the  $Fe^{III}_{LS}$  ( $S=\frac{1}{2}$ ) and  $Se^{II}_{So}$  ( $S=\frac{1}{2}$ ) and afford an  $Se^{II}_{T}$  magnetic exchange ( $Se^{II}_{So}$ ) and afford an  $Se^{II}_{T}$  magnetic spin ground state;  $Se^{II}_{So}$  and  $Se^{II}_{So}$  were estimated to be -0.16 cm<sup>-1</sup>, 0.0055 cm<sup>-1</sup>, and 1.93, respectively. AC susceptibility studies show that slow frequency-dependent SMM dynamics were operative below ca. 1.8 K (shoulders seen) and an experimental energy barrier of  $Se^{II}_{So}$  was deduced [77].

The following year two tetranuclear SMMs were reported (Fig. 10) [98, 123]. The nearly planar  $\{Fe^{III}_{2}M^{II}_{2}\}$  complexes (M<sup>II</sup> = Co, Ni) exhibit S = 2 and 3 ground states, respectively, due to antiferromagnetic and ferromagnetic exchange

between the  $[(Tp^*)Fe^{III}(CN)_3]$  and  $[cis-M^{II}(DMF)_4]$  fragments, respectively. Magnetic data analyses suggest that the squares engage in significant spin-orbit coupling and average  $g_{iso}$  values of 2.7 and 2.2, respectively [98, 123]. Frequency-dependent behavior was also seen in their AC data confirming that both are SMMs [98].

Later in 2006 a pentanuclear  $\{Fe^{III}_2Cu^{II}_3\}$  complex was shown to exhibit slow relaxation dynamics suggestive of SMM behavior. In this structure two  $[(Tp)Fe^{III}(CN)_3]$  anions are located at the apical sites of a trigonal bipyramid, which are cyanide-bridged to three five-coordinate  $[(Me_3tacn)-Cu^{II}]^{2+}$  ions that reside within equatorial plane (Fig. 4b) [109]. As before, ferromagnetic coupling between Fe<sup>III</sup> and Cu<sup>II</sup> ions was seen and an  $S_T = {}^{5/}_2$  spin ground state was found. Fitting the  $\chi T$  vs T data using an isotropic spin Hamiltonian gives g, J, and TIP values of 2.245(4), 8.5(1) cm<sup>-1</sup>, and -1.0 x  $10^{-3}$  emu/mol, respectively. The reduced magnetization data showed that appreciable anisotropy is present in

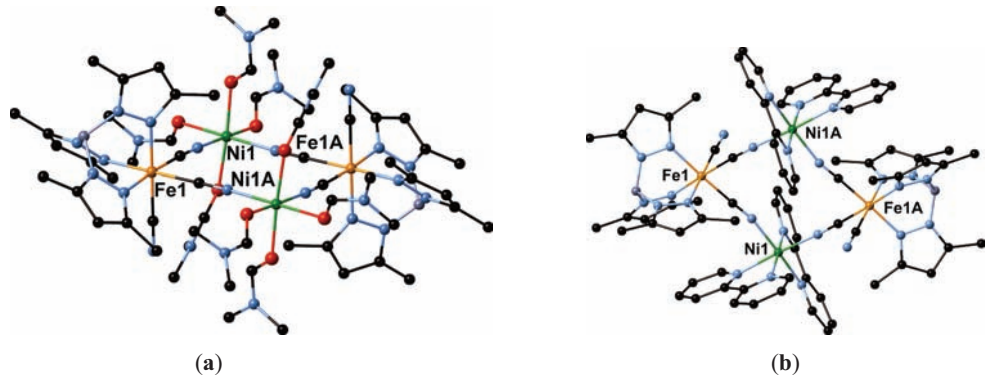


Fig. (10), (a) X-ray structure of the first {Fe<sup>III</sup>,Ni<sup>II</sup><sub>3</sub>} SMM complex. (b) X-ray structure of a ligand substituted SMM analogue.

the pentanuclear complex with D, E, and g parameters estimated to be -5.7 cm<sup>-1</sup>, 1.4 x  $10^{-3}$  cm<sup>-1</sup>, and 2.53, respectively; an SMM barrier of  $\Delta/k_{\rm B} = 23.2$  K (16 cm<sup>-1</sup>) was found. The authors suggested that the higher SMM barrier seen for the {Fe<sup>III</sup><sub>2</sub>Cu<sup>II</sup><sub>3</sub>} complex is related to the lower molecular symmetry and a linear arrangement of Fe<sup>III</sup> ions, in comparison to cubic {Fe<sup>III</sup><sub>8</sub>Cu<sup>II</sup><sub>6</sub>} [13, 77, 109-111].

# 5.2. Trinuclear Complexes

Of known tricyano-based single-molecule magnets the smallest are those with trinuclear structures. Two trinuclear SMMs have been reported to date [126, 139] and both contain a central Ni<sup>II</sup> ion that is linked to two adjacent Fe<sup>III</sup> centers via bridging cyanides (Fig. 9). In theory two structural isomers may be obtained, where the  $Fe^{III}(\mu$ -CN)Ni<sup>II</sup> units are either cis- or trans- to one another, and this tuned via ancillary ligand steric demand. The  $\{Fe^{III}_2Ni^{II}\}$  SMMs of  $\{[(pzTp)Fe^{III}(CN)_3]_2[Ni^{II}(bipy)_2]\}-2H_2O$  [126] and  $\{[(Tp^{*bn})Fe^{III}(CN)_3]_2[Ni^{II}(DMF)_4]\}$  2DMF [139] stoichiometry, contain cis- and trans- orientations of Fe<sup>III</sup>( $\mu$ -CN)Ni<sup>II</sup> units, respectively, with the iron centers related by crystallographic symmetry (Figs. 9a and 9b]. In each complex the  $Fe^{II}_{LS}(\mu\text{-CN})Ni^{II}$  bridges are nearly linear and the magnitude of the exchange coupling [ca.  $J_{iso}/k_B \sim 7.0$  K] suggests that the cyanide-mediated exchange interactions are efficient between the  $Fe^{III}_{LS}$  ( $S = \frac{1}{2}$ ) and  $Ni^{II}$  (S = 1) spin centers [126,

As judged from the magnetic data, significant magnetic anisotropy from the Fe<sup>III</sup> centers leads to the observation of SMM dynamics at low temperatures. Despite their structural differences both complexes exhibit simlar  $g_{iso}$  (ca. 2.3) and D/k<sub>B</sub> (-4.2 K) terms indicating that significant orbital contributions are present and are representative of those generally seen for many cyanide-bridged Fe<sup>III</sup>/Ni<sup>II</sup> SMMs [126, 139]. The S = 1 first excited state is ca. 14 K higher than the ground state and becomes thermally populated below ca. 2.8 K. Moreover, AC susceptibility data indicates that both complexes exhibit frequency-dependent dynamics near 2 K and effective spin reversal energy barriers ( $\Delta_{eff}$ ) of 20.6 and 17 K are found (for  $H_{dc} = 0$  Oe), respectively [126, 139].

A third trinuclear SMM was described in 2013 by Zhang [142, 143]. In this complex,  $\{[(Tp^{*Mc})Fe^{III}(CN)_3]_2[Ni^{II}(DETA)(OH_2)]\}\cdot 6H_2O\cdot MeCN$ , the  $[cis\text{-Ni}^{II}(DETA)(OH_2)(\mu\text{-}V)]$ NC)<sub>2</sub>] fragment contains a central and distorted nickel center with a tridentate mer-DETA ligand, two cis-cyanides, and a coordinated aqua ligand (Fig. 10). Extensive hydrogen bonding between lattice water and the coordinated DETA and aqua ligands were also found. A variety of close intermolecular contacts were also seen in the X-ray structure [142, 143].

Magnetic measurements show that the new complex is a third member of the trinuclear SMM class. Fitting the  $\chi T$  vs T data gave estimated values for  $J_1/k_B$  and g [+11.2(1) K and 2.41(5)] that were in the range expected for magnetic complexes with  $Fe^{III}(\mu$ -CN)Ni<sup>II</sup> units. Simulations of the M vs H data show that intermolecular antiferromagnetic interactions (inflection point) are present and a crude estimation of their magnitude (-0.28 K) was deduced [143]. At zero applied DC field, frequency-dependent magnetic relaxation was observed in the AC susceptibility data above 10 kHz, suggesting that rapid quantum tunneling (QTM) of the magnetization occurs. Anticipating that application of a small dc magnetic field would lift the degeneracy of the magnetic  $\pm m_s$ states, and concomitantly slow the rates of QTM, the AC susceptibility behavior was investigated further under the application of a static field. Indeed the rate of magnetization relaxation became slower as judged from a decrease in the characteristic frequency with increasing applied DC magnetic field strength [143].

Simulations of EPR data also confirm that the trinucelar complex exhibits axial magnetic and g tensor anisotropy [142]. The data was simulated via the following equation:

$$\widehat{H} = \mu_B \boldsymbol{B} \cdot \overleftrightarrow{g} \cdot \widehat{S} + D \widehat{S}_z^2 + E (\widehat{S}_x^2 - \widehat{S}_y^2) + B_4^0 \widehat{O}_4^0$$

where  $\mu_B$  is the Bohr magneton, B is the applied static DC magnetic field,  $\vec{g}$  is the Landé g-tensor,  $\hat{S}$  is the spinoperator, D and E are the second-order axial and rhombic zero-field splitting parameters, respectively, followed by the axial fourth-order zero-field splitting term. The EPR measurements indicate that the S = 2 complex exhibits significant g ( $g_z = 2.4$ ;  $g_y = g_x = 1.95$ ) and easy-axis magnetic anisotropy (D = -2.09 cm<sup>-1</sup>, E = 0.08,  $B_4^{\circ} = 2.3 \times 10^{-3}$  cm<sup>-1</sup>) and confirms that it is a third member of the {Fe<sup>III</sup><sub>2</sub>Ni<sup>II</sup>} SMM family [142].

A fourth trinuclear Fe<sup>III</sup>/Ni<sup>II</sup> complex was reported by Zhang and coworkers [140]. They attempted to increase the spin ground state of the {Fe<sup>III</sup><sub>2</sub>Ni<sup>II</sup>} complex by replacing diamagnetic DMF and bpy ligands with open shell ones [IM-2Py] at the Ni<sup>II</sup> site [140]. Under the assumption that efficient ferromagnetic coupling of the  $S = \frac{1}{2}$  radicals to the Ni<sup>II</sup>

centers would occur, the authors anticipated that an S=3 complex would result. Unfortunately, the paramagnetic ligands remain magnetically isolated and afforded an isotropic Curie contribution (S=1, paramagnetic) to the complex; no frequency-dependent behavior was observed in its AC susceptibility data [140]. A few other trinuclear complexes are known but they are not SMMs probably due to two factors: (1) the Fe<sup>III</sup> and Ni<sup>II</sup> centers are not efficiently coupled and/or (2) non-parallel orientations of their singleion anisotropy tensors (coincident with Fe···B axes) prevent creation of a sizable thermal barrier to magnetization reversal [126, 139, 140].

## 5.3. Tetranuclear Complexes

The dominant structural archetype when using di- and tricyano building blocks are a series of structurally related tetranuclear complexes, or molecular squares (Fig. 10). Various cationic  $\{M^n_2M^{II}_2\}^{2+}$  complexes  $(M^n = Cr^{III}, Mn^{III}, Fe^{III}, Co^{III}, VO^{2+}, TiO^{2+}; M^{II} = Mn, Co, Ni, Cu, Zn)$  [12, 13, 98-101, 103, 109-111, 129, 130, 132-134, 141] are obtained when cyanometalate and divalent salts are combined in polar media (e.g. DMF, MeOH, MeCN, etc.). The structures consist of cyanide-bridged di- and trivalent metal centers that reside in alternate corners of a molecular square, with two terminal cyanides adopting an anti orientation relative to the  $\{M^{III}(\mu\text{-CN})M^{II}\}_2$  core.

In a typical synthesis, treatment of [NEt<sub>4</sub>][(Tp\*)-M<sup>III</sup>(CN)<sub>3</sub>] (M<sup>III</sup> = Mn, Fe, Co, Cr) with divalent triflates (e.g. M<sup>II</sup> = Mn, Co, Ni, Cu) or other substitutionally labile salts in polar solvents (e.g. DMF) readily affords molecular square {M<sup>III</sup><sub>2</sub>M<sup>II</sup><sub>2</sub>} complexes [13, 98, 103, 129, 130,134, 141]. Additional squares are also known:  $\{Co^{III}_2Zn^{II}_2\}$  (S = 0) and  $\{Fe^{III}_2Zn^{II}_2\}$  (S = 1) [103],  $\{Mn^{III}_2M^{II}_2\}$  ( $M^{II} = Co$ , S = 0) 1; Ni, S = 4) [100, 101], and {[VO]<sub>2</sub>Mn<sup>II</sup><sub>2</sub>} (S = 4) [99] but none of these exhibit slow relaxation dynamics that are characteristic of SMMs. Various reports indicate that significant orbital contributions must be present at the trivalent sites within the  $\{M^{III}_{2}M^{II}_{2}\}$  complexes for the creation of a sizable SMM energy barrier [12, 98, 129-134, 141]. At least 18 square SMMs have been described with most containing [(Tp<sup>R</sup>)Fe<sup>III</sup><sub>LS</sub>(CN)<sub>3</sub>] anions, due to their magnetic anisotropy, ease of preparation, and number of known tricyano complexes (where  $Tp^R = Tp$ ,  $Tp^*$ ,  $Tp^{Me,mt3}$ ,  $Tp^{Me,mt4}$ , phTp, MeTp, iBuTp, and pzTp) (Table 2).

The first tetranuclear square SMMs were reported by Li and coworkers in 2005 [98, 123]. The nearly planar and iso  $\{[(Tp^*)Fe^{III}(CN)_3]_2[M^{II}(DMF_4]_2[OTf]_2\}\cdot 2DMF$ structural  $(M^{II} = Co, Ni)$  squares were found to exhibit S = 2 and 3 ground states, owing to local antiferromagnetic and ferromagnetic exchange, respectively (Fig. 10a). The {Fe<sup>III</sup><sub>2</sub>Co<sup>II</sup><sub>2</sub>} and {Fe<sup>III</sup><sub>2</sub>Ni<sup>II</sup><sub>2</sub>} squares exhibit significant spin-orbit coupling with  $g_{Co}$  and  $g_{Ni}$  parameters estimated to be 2.84 and 2.38, while average  $g_{iso}$  values are 2.7 and 2.2, respectively [98, 123]. Frequency-dependent behavior was seen in their AC data suggesting that both are SMMs. As judged from the magnetic data the complexes display large and negative zero-field splitting ( $D/k_B = -4.37$  and -5.73 K) and SMM barriers ( $\Delta/k_B = 17.5$  and 21.7 K) [98, 123]. Magnetic investigations on other squares show that the trivalent [(Tp\*)Fe(CN)<sub>3</sub>] centers are highly anisotropic (g = 2.9) and that they engage in antiferromagnetic (Mn<sup>II</sup> and Co<sup>II</sup>) and ferromagnetic (Ni<sup>II</sup>, Cu<sup>II</sup>) exchange, to afford S = 4, 2, 3, and 4 spin ground states, respectively [98, 123, 103].

The orientations of the magnetic anisotropy tensors within three  $\{Fe^{III}_2M^{II}_2\}$  ( $M^{II}=Mn$ , Co, Ni) complexes were investigated by Park using spin-polarized density-functional theory in 2006 [12]. She deduced that the complexes xhibit significant transverse anisotropy |E| that becomes ca. 15-36% of the longitudinal anisotropy |D|. Consistent with the magnetic data, the complexes exhibit 4-8 times the orbital contributions seen in  $Mn_{12}O_{12}(OAc)_{16}\cdot 4H_2O$ , with the total magnetic anisotropy being the difference between  $Fe^{III}/M^{II}$  pair contributions. SMM energy barriers of 22, 7, and 17.1 K were predicted for the  $\{Fe^{III}_2Mn^{II}_2\}$ ,  $\{Fe^{III}_2Co^{II}_2\}$ , and  $\{Fe^{III}_2Ni^{II}_2\}$  complexes, respectively.

The DFT studies demonstrated that easy axis anisotropy is present in the [(Tp\*)Fe<sup>III</sup>(CN)<sub>3</sub>] and [cis-Mn<sup>II</sup>(NC)<sub>2</sub>(DMF)<sub>4</sub>]<sup>2+</sup> fragments, while the Co<sup>II</sup> and Ni<sup>II</sup> ones are easy plane [12]. The calculations also suggest that contributions from the Fe<sup>III</sup> sites are highly important for generating an energy barrier, but Park later stated that efficient spin-orbit coupling (or large induced orbital angular momentum) does not always lead to large cluster magnetic anisotropy. The Fe<sup>III</sup> single-ion contributions apparently dominate the magnetic properties of the {Fe<sup>III</sup><sub>2</sub>Mn<sup>II</sup><sub>2</sub>} and {Fe<sup>III</sup><sub>2</sub>Ni<sup>II</sup><sub>2</sub>} complexes, while those arising from the Fe<sup>III</sup> and Co<sup>II</sup> centers in the {Fe<sup>III</sup><sub>2</sub>Co<sup>II</sup><sub>2</sub>} complex are nearly cancelled. In each molecular square the magnetic anisotropy appears to lie along the Fe<sup>III</sup>.···B axes, which are canted relative to the mean [Fe<sup>III</sup><sub>2</sub>(µ-CN)<sub>4</sub>M<sup>II</sup><sub>2</sub>] plane; suggesting that the single-ion anisotropy contributions originating from the Fe<sup>III</sup> sites are critical for establishing an SMM energy barrier [12, 98].

Later in 2006, Liu and coworkers reported that another square,  $\{[(Tp)Fe(CN)_3]_2[Ni(tren)]_2[ClO_4]_2\}\cdot 2H_2O$ , also exhibits frequency-dependent behavior in its AC susceptibility data [129]. The complex displays significant structural distortions, as the Ni-N-C bond angles are 161.7(3) and 173.8(3)°, respectively. Fitting the magnetic data confirmed that ferromagnetic  $Fe^{III}$  and  $Ni^{II}$  interactions lead to an S=3spin ground state and values of  $J = 4.52 \text{ cm}^{-1}$ ,  $zJ' = -0.14 \text{ cm}^{-1}$ ,  $D = -3.85 \text{ cm}^{-1}$ , and  $\Delta_{eff} = 27.2 \text{ K}$  were found for the square complex [129]. The non-linear  $Fe^{III}(\mu$ -CN)Ni<sup>II</sup> units likely led to a decrease in magnetic coupling efficiency, in comparison to more linear ones, but surprisingly, while the magnetic exchange is about half of that seen for linear cyanide bridges, the D parameters are nearly identical. As is the case with many polynuclear cyano complexes, the S=3 ground state is heavily mixed with the higher energy first excited state (S = 2) and values of D deduced from fitting of the  $\chi T$ vs T data should be considered with care [129].

The following year an additional tetranuclear square complex,  $\{[(Tp^*)Fe^{III}(CN)_3]_2[Ni^{II}(bipy)_2]_2[OTf]_2\}\cdot 2H_2O$ , was reported by Li and coworkers (Fig. **10b**) [132]. The compound was prepared *via* two synthetic methods: (1) addition of four equivalents of bpy to  $\{[(Tp^*)Fe^{III}(CN)_3]_2[Ni^{II}(DMF)_4]_2.[OTf]_2\}\cdot 2DMF$  or (2) direct combination of bpy,

Table 2. Summary of Selected SMMs Derived from  $[(Tp^R)M^n(CN)_3]^{n-4}$  Anions

cmpd.	$S_{\mathrm{T}}$	$g_{ m iso}$	$D/k_{\rm B}$ (K)	$\Delta/k_{\rm B}$ (K)	ref.
Trinuclear					
$\{[(pzTp)Fe^{III}(CN)_3]_2[Ni^{II}(bipy)_2]\}\cdot 2H_2O$	2	2.31	-5.2	20.6	126
$\{[(Tp^{*Bn})Fe^{III}(CN)_3]_2[Ni^{II}(DMF)_4]\}\cdot 2DMF$	2	2.3(1)	-4.2	16.7	139
Tetranuclear					
$\{[(Tp^*)Fe^{III}(CN)_3]_2[Co^{II}(DMF)_4]_2[OTf]_2\}\cdot 2DMF$	2	2.7	-4.37	17.5	98,123
$\{[(Tp^*)Fe^{III}(CN)_3]_2[Ni^{II}(DMF)_4]_2[OTf]_2\}\cdot 2DMF$	3	2.2	-5.73	51.5	98,123
${[(Tp^*)Fe^{III}(CN)_3]_2[Ni^{II}(bipy)_2]_2[OTf]_2}\cdot 2H_2O$	3	2.29(1)	-2.9	20.4	132
$[(Tp^{Me,mt4})Fe^{III}(CN)_3]_2[Mn^{II}(salen)]_2$	5	2.13	-0.60	13.0	144
${[(Tp)Fe^{III}(CN)_3]_2[Ni^{II}(tren)]_2[CIO_4]_2}\cdot 2H_2O$	3	2.22	-5.54	27.2	129
[(Tp <sup>Me,mt3</sup> )Fe <sup>III</sup> (CN) <sub>3</sub> ] <sub>2</sub> [Mn(Clacphmen)] <sub>2</sub>	5	2.18	-0.676	6.3(1.4)	145
$[(Tp^{Me,mt3})Fe^{III}(CN)_3]_2[Mn(5-Clsalen)]_2$	5	1.91	-1.08	7.9(3.1)	145
$[(Tp^{Me,mt3})Fe^{III}(CN)_3]_2[Mn(5-MeOsalen)]_2$	5	1.86	-1.18	7.3(4.0)	145
{[(Tp)Fe <sup>III</sup> (CN) <sub>3</sub> ] <sub>2</sub> [Ni <sup>II</sup> (R-pabn)(S-pabn)] <sub>2</sub> [PF <sub>6</sub> ] <sub>2</sub> }·2H <sub>2</sub> O·4MeCN	3	2.31(1)	-4(1)	20.3(3.0)	137
$[(^{Ph}Tp)Fe^{II}(CN)_3]_2[Ni^{II}(tren)]_2[CIO_4]_2$	3	2.284	-4.43		133
$\{[(^{Mc}Tp)Fe^{II}(CN)_3]_2[Ni^{II}(tren)]_2[ClO_4]_2\}\cdot 2H_2O$	3	2.305	-4.35		133
$\{[(^{'Bu}Tp)Fe^{II}(CN)_3]_2[Ni^{II}(tren)]_2[CIO_4]_2\} \cdot 2H_2O \cdot 2MeOH$	3	2.285	-4.68		133
$ \begin{split} \{[(Tp)Fe^{III}(CN)_3]_2[Ni^{II}(L_1)_2]_2[CIO_4]_2\}\cdot 6H_2O \\ L_1 &= 4,5\cdot[1^\prime,4^\prime] \\ \text{dithiino}[2^\prime,3^\prime-b] \\ \text{quinoxaline-2-bis(2-pyridyl)methylene-1,3-dithiole} \end{split} $	3	2.14	-4.1	8.7	136
$ \{[(^{i\text{-Bu}}Tp)Fe^{III}(CN)_3]_2[Ni^{II}(L_3)_2]_2[CIO_4]_2\} \cdot 6H_2O $ $L_3 = dimethyl \ 2 - [di(pyridin-2-yl)methylene] - 1,3 - dithiole-4,5 - dicarboxylate $	3	2.14	-4.37	13.5	136
${[(pzTp)Fe^{III}(CN)_3]_2[Ni^{II}(dpa)]_2[ClO_4]_2} \cdot 2MeOH \cdot 6H_2O$	3	2.23	2.19	20.14	134
$\{[(Tp^{*Me})Fe^{III}(CN)_3]_2[Ni^{II}(DMF)_4]_2[OTf]_2\} \cdot 2DMF$	3	2.4(1)	-	20.4	141
$\{[(Tp^{*Me})Fe^{III}(CN)_3]_2[Ni^{II}(bpy)_2]_2[CIO_4]_2\} \cdot 3MeCN \cdot 2H_2O \cdot MeOH$	3	2.5(1)	-1.8	15.7	141
Penta- and Hexanuclear				I	
$\{[(Tp)Fe^{III}(CN)_3]_2[Cu^{II}(Me_3tacn)]_3[ClO_4]_4\} \cdot 2H_2O$	5/2	2.245(4)	-8.2	23.2	109
$\{[(Tp^{4Bo})Fe^{III}(CN)_3]_2[Cu^{II}(Me_3tacn)]_3[ClO_4]_4\}\cdot 5H_2O$	5/2	2.28	-0.71		110
$\{[(Tp)Fe^{III}(CN)_3]_2[Ni^{II}(cyclen)]_3[BF_4]_4\} \cdot 4H_2O$	4	2.21	-2.4		111
$\{[(Tp)Fe^{III}(CN)_3]_4[Ni^{II}(OH_2)_2(NCMe)]_2\}\cdot 10H_2O\cdot 2MeCN$	4				112
$\{[(Tp^{*Me})Fe^{III}(CN)_3]_4[Ni^{II}(DMF)_3]_2\}\cdot 4DMF\cdot H_2O$	4	2.3(1)	-1.6	15.6	127
$\{[(pzTp)Fe^{III}(CN)_3]_4[Co^{II}(bimpy)]_2\}\cdot 2(n-PrOH)\cdot 4H_2O$	3	-	-	-	138
Octanuclear and Higher					
$\{[(pzTp)Fe^{III}(CN)_3]_4[Ni^{II}\{(pz)_3CCH_2OH\}]_4[OTf]_4\}\cdot 10DMF\cdot Et_2O$	6	2.20(5)	-0.33	11.9	125
$ \{ [(pzTp)Fe^{III}(CN)_3]_4[Ni^{II}(L_6)]_4[OTf]_4 \} \cdot 10DMF \cdot Et_2O $ $L_6 = (pz)_3C(CH_2)_6SAc $	6	2.3	-0.35	12.6	128
$\{[(pzTp)Fe^{III}(CN)_3]_4[Ni^{II}(L_{10})]_4[OTf]_4\} \cdot 10DMF \cdot Et_2O$ $L_{10} = (pz)_3C(CH_2)_{10}SAc$	6	2.3	-0.33	11.9	128
[(pzTp)Fe <sup>III</sup> (CN) <sub>3</sub> ] <sub>4</sub> [Ni <sup>II</sup> (phen)(MeOH)] <sub>4</sub> [ClO <sub>4</sub> ] <sub>4</sub> }·4H <sub>2</sub> O	6	2.45	-0.56	20.1	110

Table 2. contd....

cmpd.	$S_{\mathrm{T}}$	$g_{ m iso}$	$D/k_{\rm B}$ (K)	$\Delta/k_{\rm B}$ (K)	ref.
Octanuclear and Higher					
$\{[(Tp)Fe^{III}(CN)_3]_4[(Tp)Ni^{II}]_4\}\cdot H_2O\cdot 24MeCN$	6	1.82	-0.39	14.04	130
$\{[(Tp^{*Me})Fe^{III}(CN)_3]_4[Ni^{II}(tren)]_4[ClO_4]_4\} \cdot 7H_2O \cdot 4MeCN$	6	2.60(5)	-1.29(2)	33	135
$\{[(Tp^{*Me})Fe^{III}(CN)_{3}]_{6}[Ni^{II}(MeOH)_{3}]_{2}[Ni^{II}(MeOH)_{2}]\}\cdot 3H_{2}O\cdot 8MeOH$	6	2.5(1)	-0.7	17.7	127
$\{[(Tp)Fe^{III}(CN)_3]_8[Cu^{II}(OH_2)]_6[ClO_4]_4\} \cdot 12H_2O \cdot 2Et_2O$	7	1.93	-0.23	11.2	77

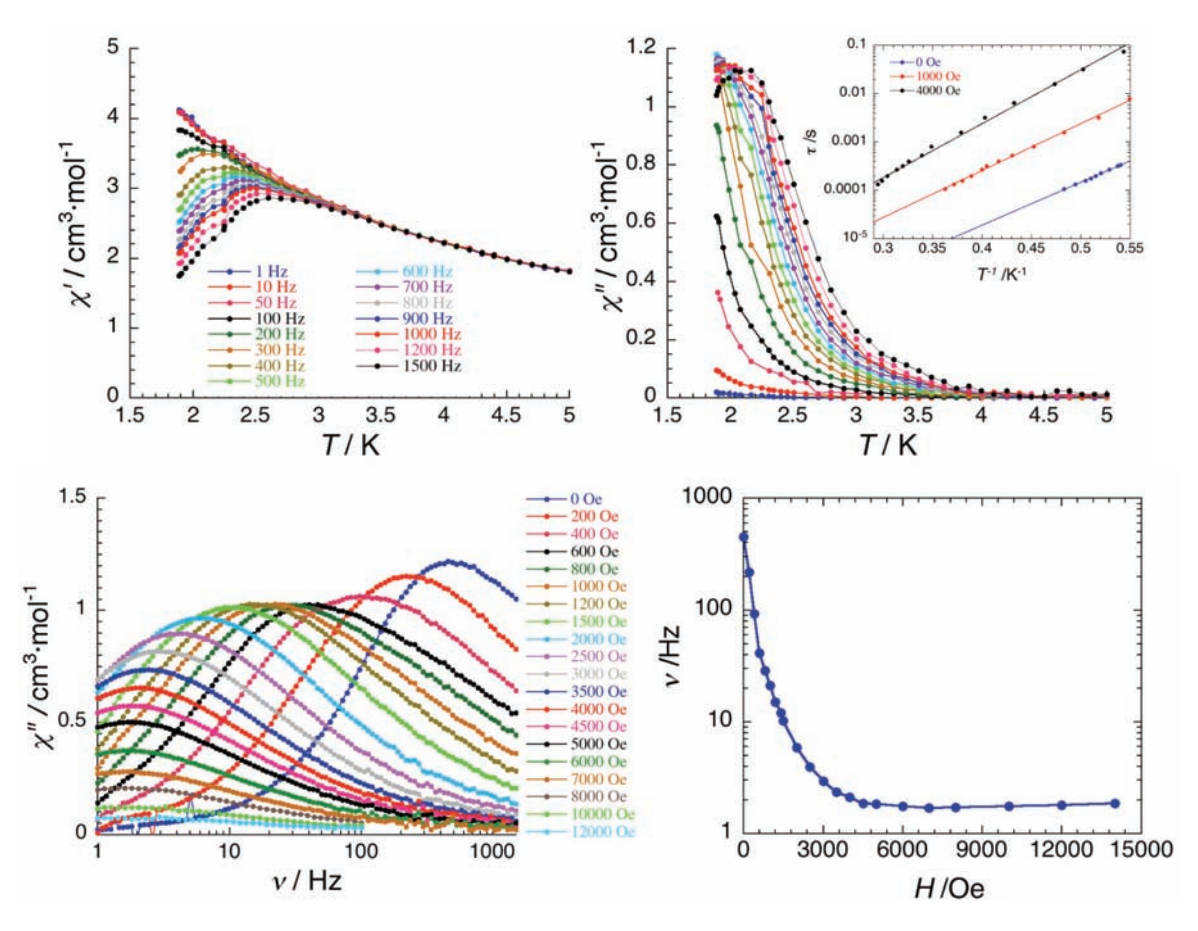


Fig. (11). Temperature dependence of real (x', top left) and imaginary (x'', top right) components of the AC susceptibility ( $H_{dc} = 0$  Oe;  $H_{ac} = 0$  Oe) for complex illustrated in Fig. (10b); Inset:  $\tau$  vs  $T^1$  plot at  $H_{dc} = 0$ , 1, and 4 kOe. Solid lines represent an Arrhenius fit of the data. Frequency dependence of x'' at 1.85 K under various applied  $H_{dc}$  (bottom left). Right: Field dependence of the characteristic frequency at 1.85 K (bottom right). Figures taken from ref. 132. Copyright 2010 Wiley.

Ni(OTf)<sub>2</sub>, and [NEt<sub>4</sub>][(Tp\*)Fe<sup>III</sup>(CN)<sub>3</sub>] in a 2:1:1 ratio. Under the initial assumption that zero-field splitting of the Ni<sup>II</sup> ions was an important and tunable factor for establishing an SMM energy barrier, the authors reasoned that ancillary ligand-induced distortions at the divalent sites would afford a systematic method for tuning {Fe<sup>III</sup><sub>2</sub>Ni<sup>II</sup><sub>2</sub>} anisotropy (Fig. **10**]. Surprisingly, the structurally distorted S = 3 complex displayed less efficient ferromagnetic exchange (J = 4.21 cm<sup>-1</sup>) and smaller D parameters (-2.9 K) indicating that the Ni<sup>II</sup> sites play a minor role in establishing an SMM energy barrier ( $\Delta_{eff} = 20.4$  K) (Fig. **11**) [12, 132].

Subsequent investigations by Wang et al. in 2008 described efforts to tune the structures and magnetic properties of three additional  $\{Fe_2Ni_2\}$  SMMs as a function of ancillary

ligand substitution at the Fe<sup>III</sup> sites [133]. For each square S=3 spin ground states and large and negative D parameters were found, ranging between -3.02 and -3.25 cm<sup>-1</sup>, indicating the presence of significant magnetic anisotropy. However, despite numerous ligand substitutions the magnetic parameters remained remarkably similar. Later in 2010, installation of chiral ligands onto the  $\{Fe^{III}_{2}Ni^{II}_{2}\}$  scaffold was reported in an attempt to prepare chiral SMMs [137]. In this complex slow relaxation behavior was observed but indications are that at least two relaxation modes are operative over the temperature range investigated. The origins of the relaxation modes remain unclear for this achiral  $\{Fe^{III}_{2}Ni^{II}_{2}\}$  square complex [137]. Later work by Zuo, Sato, and others confirm that  $\{Fe^{III}_{2}Ni^{II}_{2}\}$  squares can accommodate a variety of ancil-

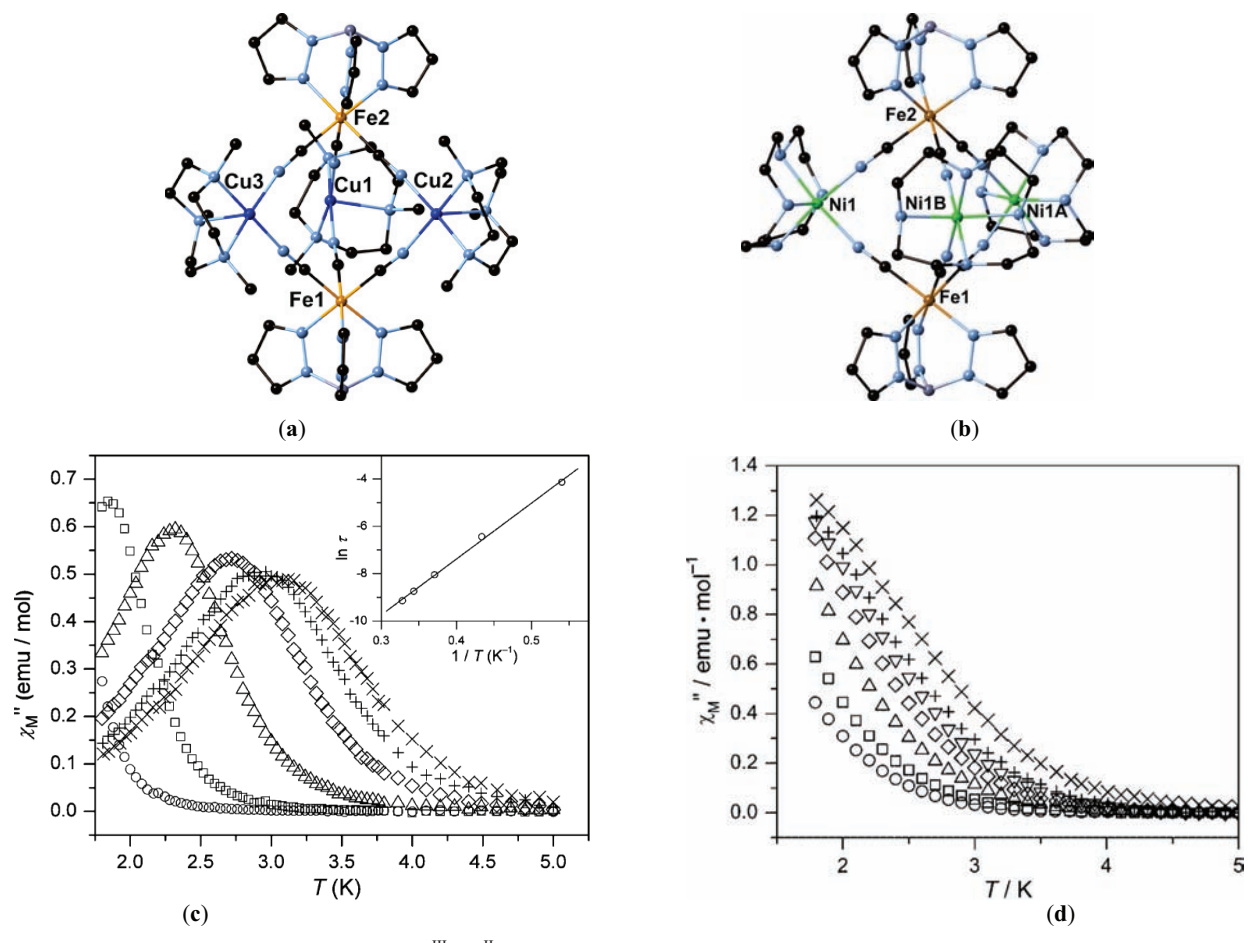


Fig. (12). (a) X-ray structures of penanuclear  $\{Fe^{III}_{2}Cu^{II}_{2}\}$  SMM complexes. (c) Temperature dependence of the out-of-phase (x'') AC susceptibility data for a. Inset: Arrhenius data for complex depicted in a. (d) Temperature dependence of the out-of-phase (x'') AC susceptibility data for complex in b. Copyright 2012 American Chemical Society [Fig. c, ref. 109] and 2007 WILEY-VCH [Fig. d, ref. 111].

lary ligands at each metal site, while simultaneously affording SMMs that exhibit a range of relaxation times and QTM rates [134, 136, 141]. In these squares structural distortions of their tetranuclear cores as well as intra- and intermolecular magnetic interactions were quantified. Through various magnetic and structural studies, the authors demonstrated that intercomplex interactions can dramatically influence the magnetic properties of structurally related complexes and proposed that these factors should be considered when designing SMMs.

Recently the structures and magnetic properties of several {Fe<sup>III</sup><sub>2</sub>Mn<sup>III</sup><sub>2</sub>} complexes containing derivatized salen supporting ligands were reported [144, 145]. In 2012 a  $[(Tp^{Me,mt4})Fe(CN)_3]_2[Mn(L)]_2$  square, where L=5-bromosalen) and  $Tp^{Me,mt4}=$  methyl tris(methyltetrahydroimadazol) borate, was reported to display an  $S_T = 5$  ground state owing to ferromagnetic interactions between the  $Fe^{III}$  (S =  $\frac{1}{2}$  and  $\mu$ -phenoxide-bridged Mn<sup>III</sup> (S = 2) centers present [144]; in this complex a modest thermal barrier to magnetization reversal [ $\Delta = 13.0$  K] was found. Hong et al. also described three additional [(Tp<sup>Me,mt3</sup>)Fe(CN)<sub>3</sub>]<sub>2</sub>[Mn(L)]<sub>2</sub> analogues, where  $Tp^{Me,mt3} = hydrotris(3-methyl-4,5-propylene-$ 5-methylpyrazol-1-yl)borate and L = Clacphmen, 5-Clsalen, and 5-MeOsalen [145]. Consistent with the presence of magnetically anisotropic  $[(Tp^{Me,mt3})Fe^{III}(CN)_3]^-$  and Jahn-Teller distorted Mn<sup>III</sup> centers  $g_{iso} \neq 2$  (1.86  $\leq g_{iso} \leq 2.18$ , small zero-field splitting (-0.676  $\leq$  D  $\leq$  -1.18 K) and rhombic terms  $(-0.42 \le E \le 0.013 \text{ cm}^{-1})$  were found [145]. Due to the presence of a crystallographic inversion center, the metal ions are related by symmetry and a parallel alignment of the Mn<sup>III</sup> Jahn-Teller and Fe<sup>III</sup>...B tensors, engenders Ising-like behavior to the complexes;  $\Delta$  ranges between 6.3 and 7.3 K [145]. The authors suggest that parallel orientation of Fe<sup>III</sup> and Mn<sup>III</sup> easy and Jahn-Teller axes, respectively, leads to the creation of an SMM energy barrier, while close intermolecular contacts decrease  $\Delta$  for the  $\{Fe_2^{III}Mn_2^{III}\}$  series [144,

### 5.4. Pentanuclear Complexes

Literature reports of pentanuclear SMMs are rare. Of known examples, all contain magnetically anisotropic  $[(Tp)Fe^{III}(CN)_3]$  anions (Fig. 12) [109-111, 131], and can be considered as structural analogues of those derived from hexacyanometalate anions [71-73, 122]. The first member of this structural archetype was reported in 2006 as a cationic trigonal bipyramidal complex of {Fe<sup>III</sup><sub>2</sub>Cu<sup>II</sup><sub>3</sub>} stoichiometry (Fig. 12a) [109]. In this complex, ferromagnetic coupling between the [(Tp)Fe<sup>III</sup>(CN)<sub>3</sub>]  $(S = \frac{1}{2})$  and Cu<sup>II</sup>  $(S = \frac{1}{2})$  centers lead to an  $S_T = 4$  ground state, and a sizable axial zerofield splitting parameter of D = -8.2 K was found. Slow magnetic relaxation dynamics were seen in its AC susceptibility data (Fig. 12c) and an SMM energy barrier of  $\Delta/k_{\rm B}$  =

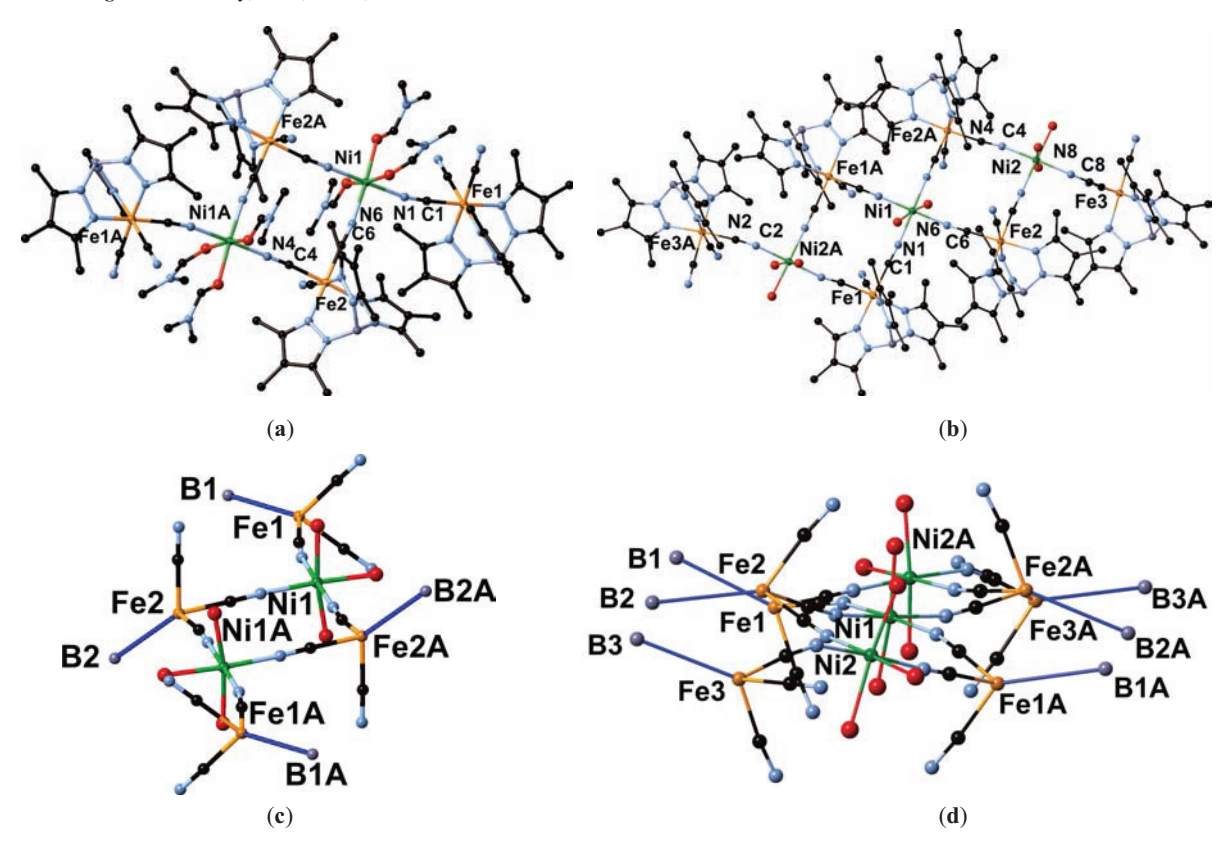


**Fig. (13).** X-ray structures of (a) hexa- and (b) nonanuclear  $\{Fe^{III}_2Ni^{II}\}_n$  complexes (n = 2, 3). (c and d) Single-ion anisotropy tensor orientations along the  $C_3$  axes  $(Fe^{III} \cdots B)$ .

23.2 K was estimated. Interestingly the direction of the molecular magnetic anisotropy was proposed to lie along the  $C_3$  axis of the molecule (Fig. 12a) [109].

Subsequent work by Zuo described the structures and magnetic properties of several additional  $\{Fe^{III}_{2}M^{II}_{3}\}$  complexes ( $M^{II}=Fe$ , Co, Ni) [131]. In each complex negative zero-field splitting terms were found via ANISOFIT [75] fiting of the reduced magnetization data, but surprisingly, no frequency-dependent behavior was seen in their AC susceptibility data. The authors proposed that molecular symmetry plays an important role in the establishing cluster anisotropy but did not provide an explanation why only the Ni<sup>II</sup> analogue displays SMM dynamics.

The following year another  $\{Fe^{III}_2Ni^II_3\}$  single-molecule magnet was reported (Fig. **12b**) [111]. The pentanuclear  $\{[(Tp)Fe^{III}(CN)_3]_2[Ni^{II}(cyclen)]_3[BF_4]_4\}\cdot 4H_2O$  cluster displayed slow dynamics (shoulders near ca. 1.8 K) in its x'' vs T data (Fig. **12d**) and fitting of the  $\chi T$  vs H data gave J=+7.8 K and g=2.21, with a TIP =  $719\times10^{-6}$  K for the integer spin ( $S_T=4$ ) complex. Subsequent fitting of the reduced magnetization data via ANISOFIT 2.0 [75] gave the following values: D=-2.4 K, E=0.02 K, and g=2.16. In comparison to  $\{Fe^{III}_2Cu^{II}_3\}$  the authors stated that the complex is an SMM, albeit with a lower effective barrier to magnetization reversal.

#### 5.5. Hexa- and Nonanuclear Complexes

The first hexanuclear  $\{Fe^{III}_2M^{II}\}_2$  complexes derived from  $[(Tp)Fe^{III}(CN)_3]^T$  units were described by Miller and coworkers in 2005 [151]. These  $\{Fe^{III}_2M^{II}\}_n$  complexes bear

structural similarities to the  $\{4,2\}$  fragments present within well-known one-dimensional cyanide-bridged ribbons of  $\{[Fe^{III}(L)(CN)_4]_2[Ni^{II}(OH_2)_2]\}\cdot 4H_2O$  (L=bpy, phen) stoichiometry. However, the authors reported that spin-glass, rather than slow dynamics that are characteristic of SMMs were seen, suggesting that another magnetic phase or unusual magnetic interactions were present. This may be due in part to the presence of coordinated and labile methanolato ligands which upon removal lead to aggregation and the formation of additional magnetic phases [127].

In 2010, Zhang et al. later described the preparation of additional structurally related SMM analogues [127]. The structures to consists of a central {Fe<sup>III</sup><sub>2</sub>M<sup>II</sup><sub>2</sub>} square whose structure is connected via two bridging cyanides to two additional [(Tp\*Me)FeIII(CN)3] fragments, that are related via an inversion center (Fig. 13a). In the same communication, a nonanuclear  $\{Fe^{III}_{6}Ni^{II}_{3}\}$  complex was reported, that consists of two corner shared  $\{Fe^{III}_{2}Ni^{II}_{2}\}$  squares sharing a common trans-[Ni<sup>II</sup>(DMF)<sub>2</sub>( $\mu$ -NC)<sub>4</sub>] unit; two cyanide-bridged [(Tp\*Me)Fe<sup>III</sup>(CN)<sub>3</sub>] ions linked to each peripheral mer- $[Ni^{II}(DMF)_3(\mu-NC)_2]$  center (Fig. 13b) [127]. The  $\{Fe^{III}_{2}Ni^{II}\}_{n}$  core of the nonanuclear complex (Fig. 13b) adopts a twisted orientation (ca. 33.1°) along the direction of the corner shared {Fe<sup>III</sup><sub>2</sub>Ni<sup>II</sup><sub>2</sub>} squares. Under the assumption that the pseudo- $C_3$  axes (Fe···B axes) are structural markers for the single-ion anisotropy tensors, the authors suggested that the hexanuclear complex has a better orientation of these in comparison to the  $\{Fe^{III}_{6}Ni^{II}_{3}\}$  complex (Figs. **9c** and **9d**).

Fitting the  $\chi T$  vs T data showed that the hexa- and nonanuclear complexes adopt  $S_T = 4$  and 6 ground states and gave

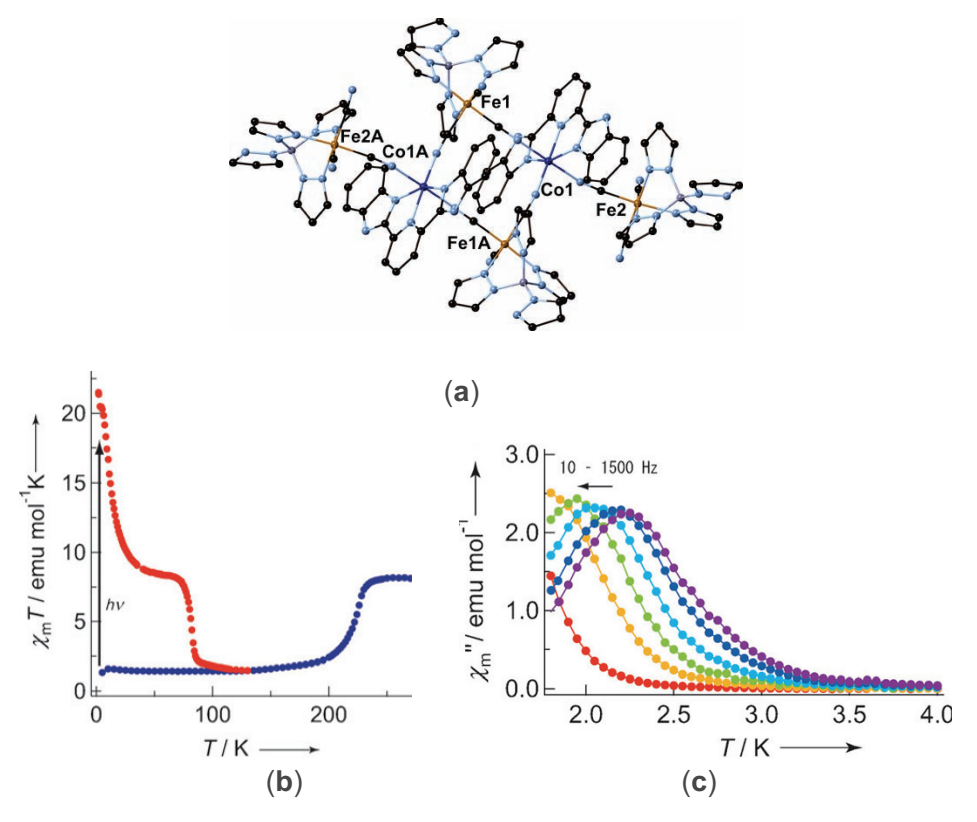


Fig. (14). (a) X-ray structure of a photomagnetic {Fe<sup>III</sup><sub>4</sub>Co<sup>II</sup><sub>2</sub>} SMM complex. (b) Magnetic data collected in the absence (•) and presence (•) of light. (c) Temperature dependence of the out-of-phase (x'') AC susceptibility data for the photostationary state. Copyright 2012 American Chemical Society (Figs. b and c) [138].

remarkably similar  $J_{\rm iso}/k_{\rm B}$  [9.0(5) and 9.0(5) K] and  $g_{\rm avg}$ [2.3(1) and 2.5(1)] parameters, respectively. Additional AC susceptibility measurements for the hexa- and nonanuclear complexes indicated that they are magnetically anisotropic, with  $D/k_{\rm B} = -1.6$  and -0.7 K and  $\Delta = 26$  and 24.5 K, respectively. The authors proposed that better alignment of the anisotropy tensors (vide supra) in the {Fe<sup>III</sup><sub>4</sub>Ni<sup>II</sup><sub>2</sub>} complex leads to greater overall magnetic anisotropy, while the larger {Fe<sup>III</sup><sub>6</sub>Ni<sup>II</sup><sub>3</sub>} one has a lower SMM barrier, owing to its twisted structure and poorly aligned  $C_3$  axes (Figs. 9c and 9d) [127].

Lastly, a {Fe<sub>4</sub>Co<sub>2</sub>} complex was reported to exhibit slow magnetization dynamics after light exposure (Fig. 14a) [138]. As is the case with many photoactive Fe/Co complexes and networks, where reversible conversion of Fe<sup>I-</sup>  $_{LS}^{I}(\mu\text{-CN})\text{Co}^{II}_{LS}$  units into Fe<sup>III</sup>  $_{LS}(\mu\text{-CN})\text{Co}^{II}_{HS}$  ones occur upon light exposure or with changing temperature, the hexanuclear complex exhibited a marked increase in its XT product upon white light exposure at 5 K (Fig. 14b). Subsequent AC susceptibility measurements suggested that the photogenerated paramagnetic {Fe<sup>III</sup><sub>4</sub>Co<sup>II</sup><sub>2</sub>} complex exhibits slow magnetic relaxation dynamics arising from the photogenerated and ferromagnetically coupled  $\mathrm{Fe}^{\mathrm{III}}_{\mathrm{LS}}(\mu\text{-CN})\mathrm{Co}^{\mathrm{II}}_{\mathrm{HS}}$ units (Fig. 14c) [138].

### 5.6. Octanuclear Complexes

Several cubic symmetry {Fe<sup>III</sup><sub>4</sub>Ni<sup>II</sup><sub>4</sub>} single-molecule magnets were reported in 2006 and 2007. In these molecular boxes the importance of intermolecular interactions and crystallographic disorder in SMM dynamics were explored in great detail (Fig. 15) [110, 125, 128, 130, 131]. In 2006, Li et al. showed that various cubes of {[(pzTp)Fe<sup>III</sup>(CN)<sub>3</sub>]<sub>4</sub>.  $[Ni^{II}(L)]_4[OTf]_4$  stoichiometry, where L = 2,2,2tris(pyrazolyl)ethanol or S(acetyl)tris(pyrazolyl)alkanes,  $(pz)_3C(CH_2)_nSAc$  (n = 3, 6, 10), could exhibit structuredependent magnetic relaxation modes as a function of alkyl chain length [125, 128]. In these complexes, two modes were seen in their AC susceptibility data above 1.8 K- only one mode exhibits field-dependent behavior and this was taken as evidence of SMM dynamics. In all complexes a second frequency-independent x'' mode was proposed to originate from close intermolecular contacts, crystallographic disorder, and/or phonon bottleneck effects [125, 128]. Of reported analogues, the  $\{{\rm Fe^{III}}_4{\rm Ni^I}_4\}$  boxes containing hydrogenbonded tris(pyrazolyl)ethanol ligands displayed the smallest x'': x' ratios (1:100), while longer alkyl chain derivatives, gave higher ones. The authors proposed that longer alkyl chains (and crystallographic disorder), gave increasingly higher magnitudes of  $\chi''$ , and ascribed these as being related to intermolecular interactions between the complexes [125, 128].

Later in 2010, Zhang and coworkers described another octanuclear complex that exhibits markedly different magnetic behavior [135]. In this complex, a central {Fe<sup>III</sup><sub>2</sub>Ni<sup>II</sup><sub>2</sub>} square is linked via a single a single bridging cyanide per Fe<sup>III</sup> site to two adjacent [cis-Ni<sup>II</sup>(tren)( $\mu$ -NC)Fe<sup>III</sup>-(CN)<sub>2</sub>(Tp\*<sup>Me</sup>)] fragments (Fig. 15b) [135]; both the cubic (Fig. 15a) and  $C_2$ -symmetric octanuclear {Fe<sup>III</sup><sub>4</sub>Ni<sup>II</sup><sub>4</sub>} complexes (Fig. 15b) contain nearly linear Ni<sup>II</sup>( $\mu$ -NC)Fe<sup>III</sup> units.

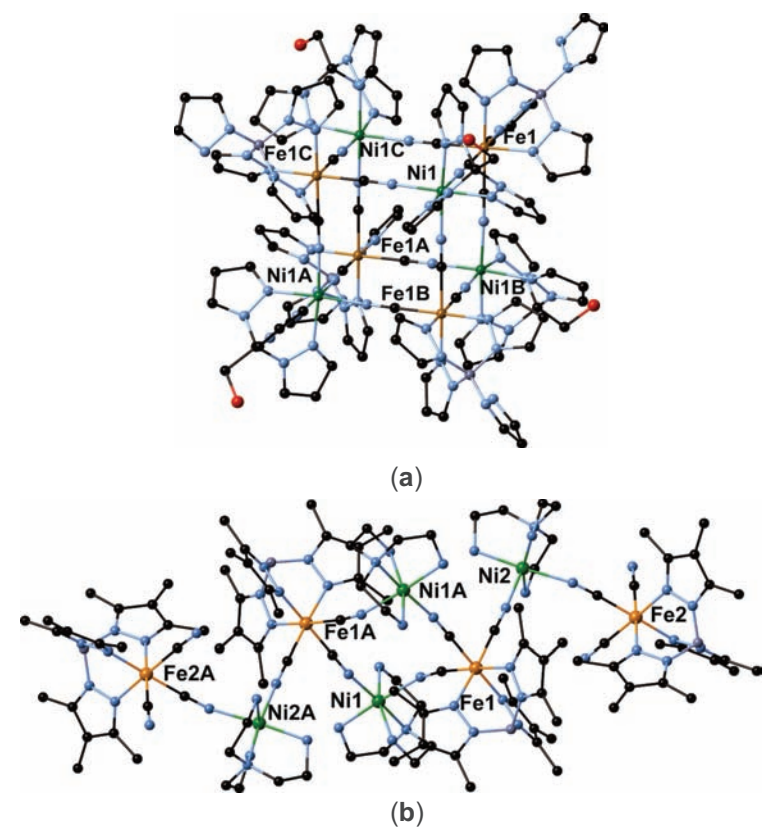
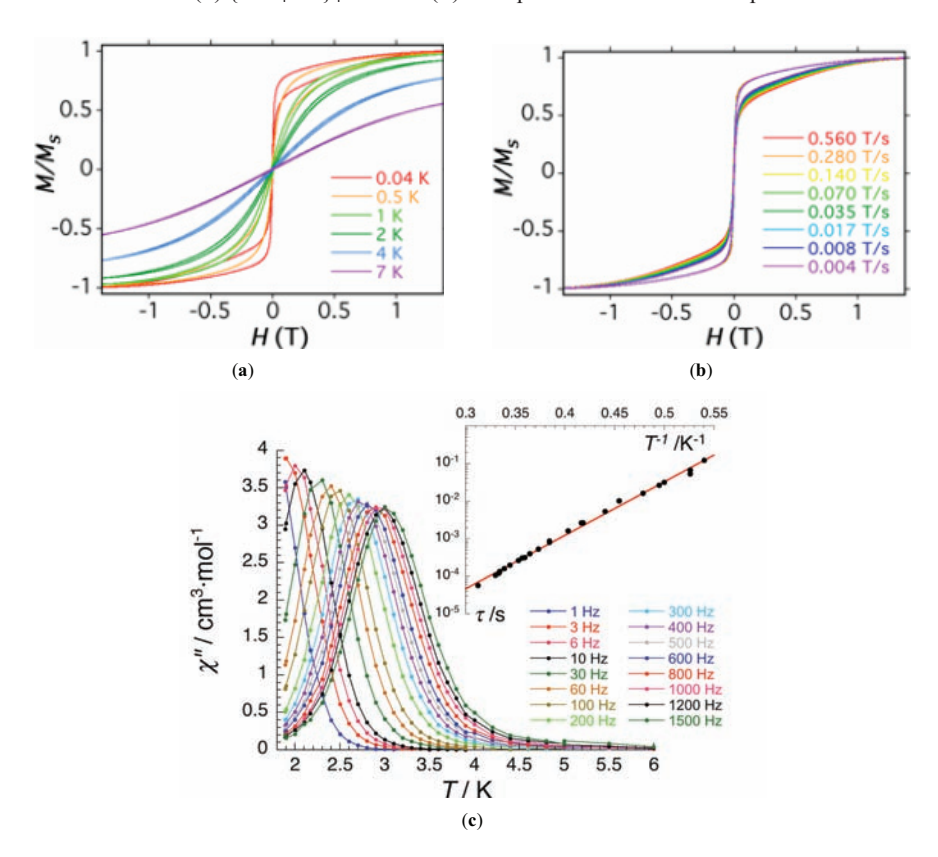
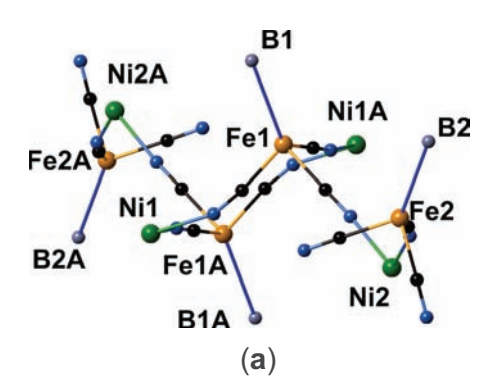


Fig. (15). X-ray structures of a molecular (a)  $\{Fe^{III}_4Ni^{II}\}_4$  box and (b) an expanded octanuclear complex.



**Fig. (16).** (**a** and **b**) μ-SQUID data for {Fe<sub>4</sub>Ni<sub>4</sub>} box in Fig. (**15a**). (**c**) x'' vs T data for {Fe<sup>III</sup><sub>4</sub>Ni<sup>II</sup><sub>4</sub>} complex in Fig. (**15b**). Inset: Semi-logarithmic  $\tau$  vs  $T^{-1}$  plot. Straight line is the data simulation via an Arrhenius law ( $\tau_0 = 2.5 \times 10^{-9}$  s). Copyright 2006 and 2011 American Chemical Society (Figs. **a** and **b**, ref. [128]) and the Royal Chemical Society (Fig. **c**, ref. [135]).



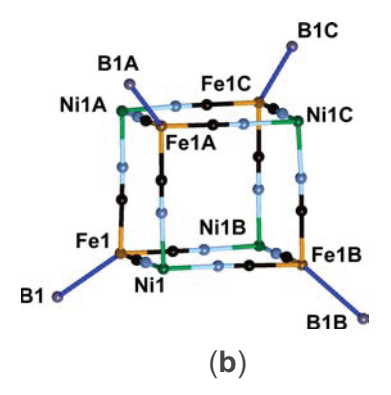


Fig. (17). (a and b) Single-ion anisotropy tensors shown (Fe. B axes) for octanuclear {Fe<sup>III</sup><sub>4</sub>Ni<sup>II</sup><sub>4</sub>} complexes (Fig. 15). Copyright 2006 and 2011 American Chemical Society (Fig. a and b, ref. [128]) and the Royal Chemical Society (Fig. c, ref. [135]).

A variety of magnetic measurements indicate that each complex adopts an  $S_T = 6$  spin ground state owing to ferromagnetic exchange between the Fe<sup>III</sup>  $(S = \frac{1}{2})$  and Ni<sup>II</sup> (S = 1)ions present. However despite having identical spin ground states dramatic differences in their experimental magnetic parameters were found, demonstrating that structural features play an important (and poorly understood) role in establishing overall magnetic anisotropy [125, 128, 135]. For example, identical exchange parameters were found, where  $J_{iso}/k_{\rm B}$ = 9.5(5) and 9.5(1) K, and fitting the  $\chi T$  vs T data leads to vastly different values for  $D/k_{\rm B}$  [-0.33(5) and -1.29(2) K] and  $g_{iso}$  [2.20(5) and 2.60(5)] [125, 128, 135], for the cubic and expanded {Fe<sup>III</sup><sub>4</sub>Ni<sup>II</sup><sub>4</sub>} complexes, respectively.

As is the case with most cyanide-based SMMs, neither complex exhibits magnetic hysteresis above 1.8 K, being consistent with rapid quantum tunneling of the magnetization. As is expected when QTM is operative, application of a small applied dc magnetic field lifts the degeneracy of the  $\pm m_s$  states, and longer relaxation times or alternatively, reductions in characteristic frequency are observed in their AC susceptibility data; both complexes exhibit this behavior confirming that efficient QTM is operative [4, 125, 135]. As judged from the sweep- and temperature dependence of the  $\mu$ -SQUID data (Fig. 16a), the cubic {Fe<sup>III</sup><sub>4</sub>Ni<sup>II</sup><sub>4</sub>} box displays rapid QTM even at mK temperatures, while the lower symmetry {Fe<sup>III</sup><sub>4</sub>Ni<sup>II</sup><sub>4</sub>} complex (Fig. **16b**) relaxes at a significantly slower rate as seen in its AC susceptibility data. Consistent with this assumption, the energy barriers were estimated to be  $\Delta/k_{\rm B} = 12$  and 33 K, respectively, with the latter being the highest reported for any 3d cyanometalate SMM [125, 128, 135].

If the SMM energy barriers are correlated with the relative orientations of their Fe...B axes (Fig. 17), then the molecular {Fe<sup>III</sup><sub>4</sub>Ni<sup>II</sup><sub>4</sub>} box probably experiences nearly complete cancellation of the orbital angular momentum originating from each Fe<sup>III</sup> center. If this assumption is correct, then the cubic {Fe<sup>III</sup><sub>4</sub>Ni<sup>II</sup><sub>4</sub>} complex experiences nearly complete cancellation of its single-ion anisotropy, leading to a small spin reversal barrier. As judged from X-ray studies, there are significant ligand steric interactions within the  $C_2$ -symmetric {Fe<sup>III</sup><sub>4</sub>Ni<sup>II</sup><sub>4</sub>} complex, which leads to a parallel alignment of the putative anisotropy tensors, and by analogy, a comparatively high  $\Delta_{eff}$  value [125, 128, 135]. If the structural requirements of building blocks can be exploited to generate polynuclear complexes with preferred orientations of their single-ion aniostropy tensors, then incorporation of sterically demanding ligands offer a means to control magnetic properties of polynuclear complexes with atom economical precision.

### 6. CONCLUSIONS AND OUTLOOK

It appears that a variety of cyanometalate-based singlemolecule magnets may be constructed using capping ligands to constrain their self-assembly towards a common structural archetype. Careful consideration of concepts such as spin state degeneracy, ancillary ligand steric interactions, and concomitantly, control of anisotropy tensor orientations in these polynuclear complexes allows for the systematic engineering of several families of SMMs with tunable magnetic properties.

Assuming that the above structure-property relationships seen for first row complexes are applicable to 4d and 5d derivatives it is conceivable that these late metal complexes may engender greater magnetic anisotropy to known structural archetypes. It follows that insertion of radially diffuse 4d and 5d ions into the corners of these SMMs will engender more efficient  $\pi$  back bonding and spin density communication. Moreover, as orbital contributions are a relativistic effect (scale with Z, atomic number), substitution of first row for late metal centers should allow for the introduction of greater single-ion anisotropy into known SMM structural archetypes [10, 11, 152-154].

We note that while several homoleptic cyanide 4d and 5d complexes, their tricyano analogues, and SMM derivatives have been reported, no pyrazolylborate counterparts are known [10, 11, 152-154]. To our knowledge [(Tp\*)NbIII-(CN)<sub>4</sub>]<sup>2-</sup> is the first in a series of late transition metal building blocks [103]. It is anticipated that by using the design principles described in this review, a better understanding of how magnetic anisotropy leads to higher energy barriers to magnetization reversal will be realized in the near future.

### CONFLICT OF INTEREST

The authors confirm that this article content has no conflicts of interest.

### **ACKNOWLEDGEMENTS**

S.M.H. acknowledges the National Science Foundation (CAREER CHE 0914935, CHE 0939987, CHE 1214063) for continuing support, the University of Missouri-St. Louis (Arts & Sciences), and the Missouri Research Board for support of research efforts. Several students are thanked for their efforts: J.R. Withers, C. Ruschman, D.F. Li, Y.Z. Zhang, U.P. Mallik, S. Brauer, M. Rhodes, H. Nguyen, M. Tang, and J. Mattingly. Several collaborators are also acknowledged for fruitful discussions and their heroic efforts over the past decade: R. Clérac, G.T. Yee, C. Mathonière, S. Hill, W. Wernsdorfer, A. Prosvirin, D. Shultz, M.H. Whangbo, G. Christou, and B.J. Hinds.

#### REFERENCES

- Leuenberger, M.N.; Loss, D. Quantum computing in molecular magnets. *Nature*, 2001, 410, 789-793.
- [2] Caneschi, A.; Gatteschi, D.; Sessoli, R.; Barra, A.L.; Brunel, L.C.; Guillot, M. Alternating Current Susceptibility, High Field Magnetization, and Millimeter Band EPR Evidence for a Ground S = 10 State in [Mn<sub>12</sub>O<sub>12</sub>(CH<sub>3</sub>COO)<sub>16</sub>(H<sub>2</sub>O)<sub>4</sub>]·2CH<sub>3</sub>COOH·4H<sub>2</sub>O. J. Am. Chem. Soc., 1991, 113, 5873-5874.
- [3] Barra, A. L.; Caneschi, A.; Cornia, A.; Fabrizi de Biani, F.; Gatteschi, D.; Sangregorio, C.; Sessoli, R.; Sorace, L. Single-Molecule Magnet Behavior of a Tetranuclear Iron(III) Complex. The Origin of Slow Magnetic Relaxation in Iron(III) Clusters. J. Am. Chem. Soc., 1999, 121, 5302-5310.
- [4] Sessoli, R.; Gatteschi, D.; Caneschi, A.; Novak, M.A. Magnetic bistability in a metal-ion cluster. *Nature*, 1993, 365, 141-143.
- [5] Wernsdorfer, W.; Aliaga-Alcalde, N.; Christou, G. Quantum Coherence in an Exchange-Coupled Dimer of Single-Molecule Magnets. *Science*, 2003, 302, 1015-1018.
- [6] Ruiz, D.; Sun, Z.; Albela, B.; Folting, K.; Ribas, J.; Christou, G.; Hendrickson, D.N. Single-Molecule Magnets: Different Rates of Resonant Magnetization Tunneling in Mn<sub>12</sub> Complexes. *Angew. Chem., Int. Ed.*, 1998, 37, 300-302.
- [7] Sessoli, R.; Gatteschi, D. Quantum Tunneling of Magnetization and Related Phenomena in Molecular Materials. *Angew. Chem., Int. Ed.* 2003, 42, 268-297, and references cited therein.
- [8] Gatteschi, D.; Sessoli, R.; Villain, J. Molecular Nano-magnets; Oxford University Press: New York, 2006, and references cited therein.
- [9] Milios, C.J.; Vinslava, A.; Wernsdorfer, W.; Moggach, S.; Parsons, S.; Perlepes, S.P.; Christou, G.; Brechin, E.K. A Record Anisotropy Barrier for a Single-Molecule Magnet. J. Am. Chem. Soc., 2007, 129, 2754-2755.
- [10] Beltran, L.M.C.; Long, J.R. Directed Assembly of Metal-Cyanide Cluster Magnets. Acc. Chem. Res., 2005, 38, 325-334.
- [11] Wang, X.Y.; Avendaño, C.; Dunbar, K.R. Molecular magnetic materials based on 4d and 5d metals. *Chem. Soc. Rev.*, 2011, 40, 3213-3238, and references cited therein.
- [12] Park, K.; Holmes, S.M. Exchange coupling and contribution of induced orbital angular momentum of low-spin Fe<sup>3+</sup> ions to magnetic anisotropy in cyanide-bridged Fe<sub>2</sub>M<sub>2</sub> molecular magnets: Spin-polarized density-functional calculations. *Phys. Rev. B*, **2006**, 74, 224440.
- [13] Wang, S.; Ding, X.H.; Zuo, J.L.; You, X.Z.; Huang, W. Tricyanometalate molecular chemistry: A type of versatile building blocks for the construction of cyano-bridged molecular architechtures. *Coord. Chem. Rev.*, 2011, 255, 1713-1732, and references cited therein.
- [14] Waldmann, O. A Criterion for the Anisotropy Barrier in Single-Molecule Magnets. *Inorg. Chem.*, 2007, 46, 10035-10037.
- [15] Nakano, M.; Oshio, H. Magnetic anisotropies in paramagnetic polynuclear metal complexes. *Chem. Rev. Soc.*, 2011, 40, 3239-3248.
- [16] Mishra, A.; Wernsdorfer, W.; Abboud, K.A.; Christou, G. Initial Observation of Magnetization Hysteresis and Quantum Tunneling in Mixed Manganese-Lanthanide Single-Molecule Magnets. *J. Am. Chem. Soc.*, 2004, 126, 15648-15649.
- [17] Karotsis, G.; Kennedy, S.; Teat, S.J.; Beavers, C.M.; Fowler, D.A.; Morales, J.J.; Evangelisti, M.; Dalgarno, S.J.; Brechin, E.K. [Mn(III)<sub>4</sub>Ln(III)<sub>4</sub>] calix[4]arene clusters as enhanced magnetic coolers and molecular magnets. *J. Am. Chem. Soc.*, 2010, 131, 12983-12990.

- [18] Peng, J.B.; Zhang, Q.C.; Kong, X.J.; Zheng, Y.Z.; Ren, Y.P.; Long, L.S.; Huang, R.B.; Zheng, L.S.; Zheng, Z. High-Nuclearity 3d-4f Clusters as Enhanced Magnetic Coolers and Molecular Magnets. J. Am. Chem. Soc., 2012, 134, 3314-3317.
- [19] Papatriantafyllopoulou, C.; Wernsdorfer, W.; Abboud, K.A.; Christou, G. Mn<sub>21</sub>Dy Cluster with a Record Magnetization Reversal Barrier for a Mixed 3d/4f Single-Molecule Magnet. *Inorg. Chem.*, 2011, 50, 421-423, and references cited therein.
- [20] Rinehart, J.D.; Long, J.R. Exploring single-ion anisotropy in the design of f-element single-molecule magnets. *Chem. Sci.*, 2011, 2, 2078-2085.
- [21] Rinehart, J.D.; Fang, M.; Evans, W.J.; Long, J.R. A N<sub>2</sub><sup>3</sup> Radical-Bridged Terbium Complex Exhibiting Magnetic Hysteresis at 14 K. J. Am. Chem. Soc., 2011, 133, 14236-14239.
- [22] Demir, S.; Zadrozny, J.M.; Nippe, M.; Long, J.R. Exchange Coupling and Magnetic Blocking in Bipyrimidyl Radical-Bridged Dilanthanide Complexes. J. Am. Chem. Soc., 2012, 134, 18546-18549
- [23] Sorace, L.; Benelli, C.; Gatteschi, D. Lanthanides in molecular magnetism: old tools in a new field. *Chem. Soc. Rev.*, 2011, 40, 3092-3104.
- [24] Guo, Y. N.; Xu, G. F.; Guo, Y.; Tang, J. Relaxation dynamics of dysprosium(III) single molecule magnets. *Dalton Trans.*, 2011, 40, 9953-9963.
- [25] Sessoli, R.; Powell, A.K. Single Molecule Magnets based on Lanthanides ions. Coord. Chem. Rev., 2009, 253, 2328, and references cited therein
- [26] Brooker, S.; Kitchen, J. A. Nano-magnetic materials: spin crossover compounds vs. single molecule magnets vs. single chain magnets. *Dalton Trans.*, 2009, 36, 7331-7340.
- [27] Habib, F.; Murugesu, M. Lessons learned from dinuclear lanthanide nano-magnets. Chem. Soc. Rev., 2013, 42, 3278-3288.
- [28] Le Roy, J.J.; Jeletic, M.; Gorelsky, S.I.; Korobkov, I.; Ungur, L.; Chibotaru, L.F.; Murugesu, M. An Organometallic Building Block Approach to Produce a Multidecker 4f Single-Molecule Magnet. J. Am. Chem. Soc., 2013, 135, 3502-3510.
- [29] Lin, P.-H.; Sun, W.-B.; Tian, Y.-M.; Yan, P.F.; Ungur, L.; Chibotaru, L.F.; Murugesu, M. Ytterbium can relax slowly too: a field-induced Yb<sub>2</sub> single-molecule magnet. *Dalton Trans.*, 2012, 41, 12349-12352.
- [30] Murugesu, M. The orientation is in the details. *Nat. Chem.*, **2012**, *4*, 347-348.
- [31] Lin, P.H.; Korobkov, I.; Burchell, T.J.; Murugesu, M. Connecting single-ion magnets through ligand dimerisation. *Dalton Trans.*, 2012, 41, 13649-13655.
- [32] Woodruff, D.N.; Winpenny, R.E.P.; Layfield, R.A. Lanthanide Single-Molecule Magnets. Chem. Rev., 2013, dx.doi.org/10.1021/cr400018q, and references cited therein.
- [33] Mougel, V.; Chatelain, L.; Pecaut, J.; Caciuffo, R.; Colineau, E.; Griveau, J.C.; Mazzanti, M. Uranium and manganese assembled in a wheel-shaped nanoscale single-molecule magnet with high spinreversal barrier. *Nat. Chem.*, 2012, 4, 1011-1017.
- [34] Antunes, M. A.; Pereira, L. C.J.; Santos, I.C.; Mazzanti, M.; Marcalo, J.; Almeida, M. [U(Tp<sup>Me2</sup>)<sub>2</sub>(bipy)]<sup>†</sup>: A Cationic Uranium(III) Complex with Single-Molecule-Magnet Behavior. *Inorg. Chem.*, **2011**, *50*, 9915-9917.
- [35] Mills, D.R.; Moro, F.; McMaster, J.; van Slageren, J.; Lewis, W.; Blake, A.J.; Liddle, S.T. A delocalized arene-bridged diuranium single-molecule magnet. *Nat. Chem.*, 2011, 3, 454-460.
- [36] Rinehart, J.D.; Meihaus, K.R.; Long, J.R. Observation of a Secondary Slow Relaxation Process for the Single-Molecule Magnet U(H<sub>2</sub>BPz<sub>2</sub>)<sub>3</sub>. J. Am. Chem. Soc., 2010, 132, 7572-7573.
- [37] Magnani, N.; Apostolidis, C.; Morgernstern, A.; Colineau, E.; Griveau, J.C.; Bolvin, H.; Walter, O.; Caciuffo, R. Magnetic Memory Effect in a Transuranic Mononuclear Complex. *Angew. Chem., Int. Ed.*, 2011, 50, 1696-1698.
- [38] Rinehart, J.D.; Long, J.R. Slow Magnetic Relaxation in a Trigonal Prismatic Uranium(III) Complex. J. Am. Chem. Soc., 2010, 131, 12558-12559.
- [39] Rinehart, J.D.; Long, J.R. Slow magnetic relaxation in homoleptic trispyrazolylborate complexes of neodymium(III) and uranium(III). *Dalton. Trans.*, 2012, 41, 13572-13574.
- [40] Harman, W.H.; Harris, T.D.; Freedman, D.E.; Fong, H.; Chang, A.; Rinehart, J.D.; Ozarowski, A.; Sougrati, M.T.; Grandjean, F.; Long, G.J.; Long, J.R.; Chang, C.J. Slow Magnetic Relaxation in a

- Family of Trigonal Pyramidal Iron(II) Pyrrolide Complexes. J. Am. Chem. Soc., 2010, 132, 18115-18126.
- [41] Atanasov, M.; Zadrozny, J.M.; Long, J.R.; Neese, F. A theoretical analysis of chemical bonding, vibronic coupling, and magnetic anisotropy in linear iron(II) complexes with single-molecule magnet behavior. Chem. Sci., 2013, 4, 139-156.
- [42] Zadrozny, J.M.; Atansov, M.; Bryan, A.M.; Lin, C.Y.; Rekken, B.D.; Power, P.P.; Long, J.R. Slow magnetization dynamics in a series of two-coordinate iron(II) complexes. Chem. Sci., 2013, 4,
- Freedman, D.E.; Harman, W.H.; Harris, T.D.; Long, G.J.; Chang, [43] C.J.; Long, J.R. Slow Magnetic Relaxation in a High-Spin Iron(II) Complex. J. Am. Chem. Soc., 2010, 132, 1224-1225.
- [44] Lin, P.H.; Smythe, N.C.; Gorelsky, S. I.; Maguire, S.; Henson, N.J.; Korobkov, I.; Scott, B.L.; Gordon, J.C.; Baker, R.T.; Murugesu, M. Importance of Out-of-State Spin-Orbit Coupling for Slow Magnetic Relaxation in Mononuclear Fe<sup>II</sup> Complexes. J. Am. Chem. Soc., **2011**, *133*, 15806-15809.
- [45] Palii, A.V.; Clemente-Juan, J.M.; Coronado, E.; Klokishner, S.I.; Ostrovsky, S.M.; Reu, O.S. Role of Orbital Degeneracy in the Single Molecule Magnet Behavior of a Mononuclear High-Spin Fe(II) Complex. Inorg. Chem., 2010, 49, 8073-8077.
- [46] Jurca, T.; Farghal, A.; Lin, P.H.; Korobkov, I.; Murugesu, M.; Richeson, D.S. Single-Molecule Magnetic Behavior with a Single Metal Center Enhanced through Peripheral Ligand Modification. J. Am. Chem. Soc., 2011, 133, 15814-15817.
- [47] Reiff, W.M.; LaPointe, A.M.; Witten, E.H. Virtual Free-ion Magnetism and the Absence of Jahn-Teller Distortion in a Linear Two-Coordinate Complex of High-Spin Iron(II). J. Am. Chem. Soc., 2004, 126, 10206-10207.
- [48] Merrill, W.A.; Stich, T.A.; Brynda, M.; Yeagle, G.J.; Fettinger, J.C.; De Hont, R.; Reiff, W.M.; Schulz, C.E; Britt, R.D.; Power, P.P. Direct Spectroscopic Observation of Large Quenching of First-Order Orbital Angular Momentum with Bending in Monomeric, Two-Coordinate Fe(II) Primary Amido Complexes and the Profound Magnetic Effects of the Absence of Jahn-Teller and Renner-Teller Distortions in Rigorously Linear Coordination. J. Am. Chem. Soc., 2009, 131, 12693-12702
- [49] Reiff, W.M.; Schulz, C.E.; Whangbo, M.H.; Seo, J.I.; Lee, Y.S.; Potraz, G.R.; Spicer, C.W.; Girolami, G.S. Consequences of a Linear Two-Coordinate Geometry for the Orbital Magnetism and Jahn-Teller Distortion Behavior of the High Spin Iron(II) Complex Fe[N(t-Bu)<sub>2</sub>]<sub>2</sub>. J. Am. Chem. Soc., 2009, 131, 404-405.
- [50] Zadrozny, J.M.; Xiao, D.J.; Atanasov, M.; Long, G.L.; Grandjean, F.; Neese, F.; Long, J.R. Magnetic blocking in a linear iron(I) complex. Nat. Chem., 2013, DOI: 10.1038/NCHEM.1630.
- [51] Andres, H.; Bominaar, E.L.; Smith, J.M.; Eckert, N.A.; Holland, P.L.; Münck, E. Planar Three-Coordinate High-Spin Fe<sup>II</sup> Complexes with Large Orbital Angular Momentum: Mössbauer, Electron Paramagnetic Resonance, and Electronic Structure Studies. J. Am. Chem. Soc., 2002, 124, 3012-3025.
- [52] Holland, P.L. Electronic Structure and Reactivity of Three-Coordinate Iron Complexes. Acc. Chem. Res., 2008, 41, 905-914.
- Krzystek, J.; Swenson, D.C.; Zvyagin, S.A.; Smirnov, D.; Ozarowski, A.; Telser, J. Cobalt(II) "Scorpionate" Complexes as [53] Models for Cobalt-Substituted Zinc Enzymes: Elelctronic Structure Investigation by High-Frequency and -Field Electron Paramagnetic Resonance Spectroscopy. J. Am. Chem. Soc., 2010, 132, 5241-
- Zadrozny, J.M.; Liu, J.; Piro, N.A.; Chang, C.J.; Hill, S.; Long, J.R. [54] Slow magnetic relaxation in a pseudotetrahedral cobalt(II) complex with easy-plane anisotropy. Chem. Commun., 2012, 48, 3927-3929.
- [55] Zadrozny, J.M.; Long, J.R. Slow Magnetic Relaxation at Zero Field in the Tetrahedral Complex [Co(SPh)<sub>4</sub>]<sup>2</sup>. J. Am. Chem. Soc., 2011, 133, 20732-20734.
- Titiš, J.; Boca, R. Magnetostructural D Correlation in Nickel(II) [56] Complexes: Reinvestigation of the Zero-Field Splitting. Inorg. Chem., 2010, 49, 3971-3973.
- [57] Desrochers, P.J.; Telser, J.; Zvyagin, S.A.; Ozarowski, A.; Krzystek, J.; Vicic, D. A. Electronic Structure of Four-Coordinate  $C_{3v}$ Nickel(II) Scorpionate Complexes: Investigation by High-Frequency and -Field Electron Paramagnetic Resonance and Elelctronic Absorption Spectroscopies. Inorg. Chem., 2006, 45, 8930-8941.
- [58] Trofimenko, S.; Calabrese, J.C.; Kochi, J.K.; Wolowiec, S.; Hulsbergen, F.B.; Reedijk, J. Spectroscopic Analysis, Coordination

- Chemistry, and X-ray Structures of Nickel(II) Compounds with Sterically Demanding Tris(pyrazolyl)borate Ligands and Azide or (Thio)cyanate Anions. Crystal and Molecular Structures of Bis(uthiocyanatoN,S)(hydridotris(3-isopropyl-4-bromopyrazol-1yl)borate)nickel(II)]-3-Heptane and (Thiocyanato-N)(hydriotris(3tert-butyl-5-methylpyrazol-1-yl)borate)nickel(II). Inorg. Chem., 1992, 31, 3943-3950.
- [59] Entley, W.R.; Girolami, G.S. High-Temperature Molecular Magnets Based on Cyanovanadate Building Blocks: Spontaneous Magnetization at 230 K. Science, 1995, 268, 397-400.
- Hatlevik, Ø.; Buschmann, W.E.; Zhang, J.; Manson, J.L.; Miller, [60] J.S. Enhancement of the Magnetic Ordering Temperature and Air Stability of a Mixed Valent Vanadium Hexacyanochromate(III) Magnet to 99 °C (372 K). Adv. Mater., 1999, 11, 914-918.
- [61] Ferlay, S.; Mallah, T.; Ouahès, R.; Veillet, P.; Verdaguer, M.A room-temperature organometallic magnet based on Prussian blue. Nature, 1995, 378, 701-703.
- [62] Holmes, S.M.; Girolami, G.S. Sol-Gel Synthesis of KV<sup>II</sup>[Cr<sup>III</sup>(CN)<sub>6</sub>]·2H<sub>2</sub>O: A Crystalline Molecule-Based Magnet with a Magnetic Ordering Temperature above 100 °C. J. Am. Chem. Soc., 1999, 121, 5593-5594.
- Verdaguer, M.; Bleuzen, A.; Marvaud, V.; Vaissermann, J.; Seuleiman, M.; Desplanches, C.; Scuiller, A.; Train, C.; Garde, R.; Gelly, G.; Lomenech, C.; Rosenman, I.; Veillet, P.; Cartier, C.; Villain, F. Molecules to build solids: high T<sub>c</sub> molecule-based magnets by design and recent revival of cyano complexes chemistry. Coord. Chem. Rev., 1999, 190-192, 1023-1047, and references cited therein.
- [64] Verdaguer, M.; Girolami, G.S. Magnetoscience: molecules to materials, vol. V (eds Miller, J.S.; Drillon, M.); Wiley: Weinheim, Germany, and references cited therein.
- [65] Kahn, O. Molecular Magnetism; VCH Publishers: New York, 1992.
- Carlin, R.L. Magnetochemistry; Springer-Verlag: New York, 1986.
- [67] Boudreaux, E.A.; Mulay, L.N. Theory and Applications of Molecular Paramagnetism; John Wiley and Sons: New York, 1976.
- [68] Goodenough, J. Magnetism and the Chemical Bond, Wiley: New
- [69] Gatteschi, D.; Kahn, O.; Miller, J.S.; Palacio, F., Eds. Magnetic Molecular Materials, Kluwer: Dordrecht, 1991.
- [70] Shores, M.P.; Long, J.R. Tetracyanide-Bridged Divanadium Complexes: Redox Switching between Strong Antiferromagnetic and Strong Ferromagnetic Coupling. J. Am. Chem. Soc., 2002, 124, 3512-3513.
- [71] Dunbar, K.R.; Schelter, E.J.; Palii, A.V.; Ostrovsky, S.M.; Mirovitskii, V.Y.; Hudson, J.M.; Omary, M.A.; Klokishner, S.I.; Tsukerblat, B.S. Unusual Magnetic Behavior of Six-Coordinate, Mixed-Ligand Re(II) Complexes: Origin of a Strong Temperature-Independent Paramagnetism. J. Phys. Chem. A, 2003, 107, 11102-11111.
- Berlinguette, C.P.; Vaughn, D.; Cañada-Vilalta, C.; Galán-[72] Mascarós, J. R.; Dunbar, K. R. A Trigonal-Bipyramidal Cyanide Cluster with Single-Molecule-Magnet Behavior: Synthesis, Structure, and Magnetic Properties of {Mn<sup>II</sup>(tmphen)<sub>2</sub>]<sub>3</sub>[Mn<sup>III</sup>(CN)<sub>6</sub>]<sub>2</sub>}. Angew. Chem., Int. Ed. 2003, 42, 1523-1526.
- Palii, A.V.; Ostrovsky, S.M.; Klokishner, S.I.; Tsukerblat, B.S.; Berlinguette, C.P.; Dunbar, K.R.; Galán-Mascarós, J.R. Role of the Orbitally Degenerate Mn(III) Ions in the Single-Molecule Magnet Behavior of the Cyanide Cluster {Mn<sup>II</sup>(tmphen)<sub>2</sub>]<sub>3</sub>[Mn<sup>III</sup>(CN)<sub>6</sub>]<sub>2</sub>} (tmphen = 3,4,7,8-tetramethyl-1,10-phenthroline). J. Am. Chem. Soc., 2004, 126, 16860-16867.
- Sokol, J.J.; Hee, A.G.; Long, J.R. A Cyano-Bridged Single-[74] Molecule Magnet: Slow Relaxation in a Trigonal Prismatic MnMo<sub>6</sub>(CN)<sub>18</sub> Cluster. J. Am. Chem. Soc., 2002, 124, 7656-7657.
- Shores, M.P.; Sokol, J.J.; Long, J.R. Nickel(II)-Molybdenum(III)-[75] Cyanide Clusters: Synthesis and Magnetic Behavior of Species Incorporating [(Me3tacn)Mo(CN)3]. J. Am. Chem. Soc., 2002, 124,
- [76] Schelter, E.J.; Bera, J.K.; Basca, J.; Galán-Mascarós, J.R.; Dunbar, K.R. New Paramagnetic Re(II) Compounds with Nitrile and Cyanide Ligands Prepared by Homolytic Scission of Dirhenium Complexes. Inorg. Chem., 2003, 42, 4256-4258.
- Wang, S.; Zuo, J.J.; Zhou, H.C.; Choi, H.J.; Ke, Y.; Long, J.R.; You, X.Z.  $[(Tp)_8(H_2O)_6Cu^{II}_6Fe^{III}_8(CN)_{24}]^{4+}$ : A Cyanide-Bridged Face-Centered-Cubic Cluster with Single-Molecule-Magnet Behavior. Angew. Chem., Int. Ed., 2004, 43, 5940-5943.

- [78] Schelter, E.J.; Prosvirin, A.V.; Dunbar, K.R. Molecular Cube of Re<sup>II</sup> and Mn<sup>II</sup> That Exhibits Single-Molecule Magnetism. *J. Am. Chem. Soc.*, 2004, 126, 15004-15005.
- [79] Schelter, E.J.; Prosvirin, A.V.; Reiff, W.M.; Dunbar, K.R. Unusual Magnetic Metal-Cyanide Cubes of Re<sup>II</sup> with Alternating Octahedral and Tetrahedral Corners. *Angew. Chem., Int. Ed.*, 2004, 43, 4912-4915.
- [80] Trofimenko, S. Scorpionates, The Coordination Chemistry of Polypyrazolylborate Ligands; Imperial College Press: London, 1999, and references cited therein.
- [81] Trofimenko, S.; Long, J.R.; Nappier, T.; Shore, S.G. Some Significant Compounds of Boron. *Inorg. Synth.*, 1970, 12, 99-107.
- [82] Trofimenko, S. Boron-Pyrazole Chemistry. IV. Carbon- and Boron-Substituted Poly(1-pyrazolyl)borates. J. Am. Chem. Soc., 1967, 89 6288-6294
- [83] Trofimenko, S. Recent Advances in Poly(pyrazolyl)borate (Scorpionate) Chemistry. Chem. Rev., 1993, 93, 943-980.
- [84] Trofimenko, S. Transition Metal Polypyrazolylborates Containing Other Ligands. J. Am. Chem. Soc., 1969, 91, 588-595.
- [85] Trofimenko, S. Transition Metal Poly(1-pyrazolyl)borates Containing Other Ligands. J. Am. Chem. Soc., 1967, 89, 3903-3904.
- [86] Mashima, K.; Oshiki, T.; Tani, K. Tp\*Sn(Cl)Bu<sub>2</sub> as a Convenient Reagent for the Preparation of Hydridotris(3,5-dimethylpyrazolyl)borate Complexes of Niobium, Tantalum, and Zirconium. Organometallics, 1997, 16, 2760-2762.
- [87] Trofimenko, S.; Long, J.R.; Nappier, T.; Shore, S.G. Some Significant Compounds of Boron. *Inorg. Synth.*, 1970, 12, 99-107.
- [88] Trofimenko, S. Boron-Pyrazole Chemistry. IV. Carbon- and Boron-Substituted Poly(1-pyrazolyl)borates. J. Am. Chem. Soc., 1967, 89, 6288-6294.
- [89] Trofimenko, S. Transition Metal Poly(1-pyrazolyl)borates Containing Other Ligands. J. Am. Chem. Soc., 1967, 89, 3903-3904.
- [90] Brunker, T.J.; Hascall, T.; Cowley, A.R.; Rees, L.H.; O'Hare, D. Variable Coordination Modes of Hydrotris(3-isopropyl-4-bromopyrazolyl)borate (Tp') in Fe(II), Mn(II), Cr(II), and Cr(III) Complexes: Formation of Tp'Cl (M = Fe and Mn), Structural Isomerism in CrTp 2, and the Observation of Tp' as an Uncoordinated Anion. *Inorg. Chem.*, 2001, 40, 3170-3176.
- [91] Trofimenko, S. Anomalous Reactions of Sterically Hindered Molybdenum Carbonyl Anions. *Inorg. Chem.*, 1971, 10, 504-507.
- [92] Millar, M.; Lincoln S.H.C.J.S.S.; Koch, S.A. Stable Monomeric Complexes of Molybdenum(III) and Tungsten(III). J. Am. Chem. Soc., 1982, 104, 288-289.
- [93] Mashima, K.; Oshiki, T.; Tani, K. Tp\*Sn(Cl)Bu<sub>2</sub> as a Convenient Reagent for the Preparation of Hydridotris(3,5-dimethylpyrazolyl)borate Complexes of Niobium, Tantalum, and Zirconium. Organometallics, 1997, 16, 2760-2762.
- [94] Hubert-Pfalzgraf, L.G.; Tsunoda, M. Synthesis and Characterization of Niobium(V) and Niobium(IV) Poly(1-pyrazolyl)borates. Polyhedron, 1983, 2, 203-210.
- [95] Kikichi, S.; Sasakura, Y.; Yoshizawa, M.; Ohzu, Y.; Moro-oka, Y.; Akita, M. Selective Synthesis, Characterization, and Configurational Flexibility of the Coordinatively Unsaturated Metal Center of Half-Sandwich Type Complexes with the Less-Hindered Hydrotris(3,5-dimethyl-4-X-1-pyrazolyl)borate Ligands [Tp<sup>Me2,X-Mi(k²-O,O'-L)]</sup> (M = Ni, Co; L = NO<sub>3</sub>, OAc; X = Me, H, Br). Bull. Chem. Soc. Jpn., 2002, 75, 1255-1262.
- [96] Reger, D.L.; Collins, J.E.; Rheingold, A.L.; Liable-Sands, L.M. Solid State Structure of {[HC(3,5-Me<sub>2</sub>pz)<sub>3</sub>][HB(3,5-Me<sub>2</sub>pz)<sub>3</sub>]Cd}-{B[3,5-(CF<sub>3</sub>)<sub>2</sub>C<sub>6</sub>H<sub>3</sub>]<sub>4</sub>}: Comparison of the Bonding of Tris-(pyrazolyl)methane and Tris(pyrazolyl)borate Ligands. *Inorg. Chem.*, **1999**, *38*, 3235-3237.
- [97] Lescouëzec, R.; Vaissermann, J.; Lloret, F.; Julve, F.; Verdaguer, M. Ferromagnetic Coupling between Low- and High-Spin Iron(III) Ions in the Tetranuclear Complex fac-{[Fe<sup>III</sup>{HB(pz)<sub>3</sub>}{CN)<sub>2</sub>]<sub>3</sub>. Fe<sup>III</sup>(H<sub>2</sub>O)<sub>3</sub>}·6H<sub>2</sub>O ([HB(pz)<sub>3</sub>] = Hydrotris(1-pyrazolyl)borate). Inorg. Chem., 2002, 41, 5943-5945.
- [98] Li, D.; Parkin, S.; Wang, G.; Yee, G.T.; Prosvirin, A.V.; Holmes, S.M. Single Molecule Magnets Constructed from Cyanometalates: {Tp\*Fe<sup>III</sup>(CN)<sub>3</sub>M<sup>II</sup>(DMF)<sub>4</sub>]<sub>2</sub>[OTf]<sub>2</sub>}·2DMF (M<sup>II</sup> = Co, Ni). *Inorg. Chem.*, **2005**, *44*, 4903-4905.
- [99] Li, D.; Parkin, S.; Wang, G.; Yee, G.T.; Holmes, S.M. Early Metal Di- and Tricyanometalates: Useful Building Blocks for Constructing Magnetic Clusters. *Inorg. Chem.*, 2006, 45, 2773-2775.
- [100] Tang, M.; Li, D.; Mallik, U.P.; Withers, J.R.; Brauer, S.; Rhodes, M. R.; Clérac, R.; Yee, G.T.; Whangbo, M.W.; Holmes, S.M. First

- Structurally Characterized Tricyanomanganate(III) and its Magnetic {Mn<sup>III</sup><sub>2</sub>Mn<sup>II</sup><sub>2</sub>} Complexes (M<sup>II</sup> = Mn, Ni). *Inorg. Chem.*, **2010**, 49, 4753-4755.
- [101] Tang, M.; Li, D.; Mallik, U.P.; Zhang, Y.Z.; Clérac, R.; Holmes, S.M. Synthesis and Characterization of Di- and Trivalent Pyrazolylborate β-Diketonates and Cyanometalates. *Inorg. Chem.*, 2011, 50, 5153-5164.
- [102] Li, D.; Ruschman, C.; Parkin, S.; Clerac, R.; Holmes, S.M. Syntheses, structures, and magnetic characterization of dicyanometalate(II) building blocks: [NEt<sub>4</sub>][(Tp\*)M<sup>II</sup>(CN)<sub>2</sub>] [M<sup>II</sup> = Cr, Co, Ni; Tp\* = hydridotris(3,5-dimethylpyrazol-1-yl)borate]. *Chem. Commun.*, **2006**, *38*, 4036-4038.
- [103] Unpublished results.
- [104] Heinrich, J.L.; Sokol, J.J.; Hee, A.G.; Long, J.R. Manganese-Chromium-Cyanide Clusters: Molecular MnCr<sub>6</sub>(CN)<sub>18</sub> and Mn<sub>3</sub>Cr<sub>6</sub>(CN)<sub>18</sub> Species and a Related MnCr<sub>3</sub>(CN)<sub>9</sub> Chain Compound. J. Solid St. Chem., 2001, 159, 293-301.
- [105] Heinrich, J.L.; Berseth, P.A.; Long, J.R. Molecular Prussian Blue analogues: synthesis and structure of cubic Cr<sub>4</sub>Co<sub>4</sub>(CN)<sub>12</sub> and Co<sub>8</sub>(CN)<sub>12</sub> clusters. *Chem. Commun.*, **1998**, *11*, 1231-1232.
- [106] Berseth, P.A.; Sokol, J.J.; Shores, M.P.; Heinrich, J.L.; Long, J.R. High-Nuclearity Metal-Cyanide Clusters: Assembly of a Cr<sub>8</sub>Ni<sub>6</sub>(CN)<sub>24</sub> Cage with a Face-Centered Cubic Geometry. *J. Am. Chem. Soc.*, 2000, 122, 9655-9662.
- [107] Sokol, J.J.; Shores, M.P.; Long, J.R. High-Nuclearity Chromium-Nickel-Cyanide Clusters: An Open  $Cr_8Ni_5(CN)_{24}$  Cage and a  $C_3$ -Symmetric  $Cr_{10}Ni_9(CN)_{42}$  Cluster Incorporating Three Forms of Cyanonickelate. Angew. *Chem., Int. Ed.*, **2001**, *40*, 236-239.
- [108] Sokol, J.J.; Shores, M.P.; Long, J.R. Giant Metal-Cyanide Coordination Clusters: Tetracapped Edge-Bridged Cubic Cr<sub>12</sub>Ni<sub>12</sub>(CN)<sub>48</sub> and Double Face-Centered Cubic Cr<sub>14</sub>Ni<sub>13</sub>(CN)<sub>48</sub> Species. *Inorg. Chem.*, 2002, 41, 3052-3054.
- [109] Wang, C.F.; Zuo, J.L.; Bartlett, B.M.; Song, Y.; Long, J.R.; You, X.Z. Symmetry-Based Magnetic Anisotropy in the Trigonal Bipyramidal Cluster [Tp(Me<sub>3</sub>tacn)<sub>3</sub>Cu<sub>3</sub>Fe<sub>2</sub>(CN)<sub>6</sub>]<sup>4+</sup>. J. Am. Chem. Soc., 2006, 128, 7162-7163.
- [110] Gu, Z.G.; Liu, W.; Yang, Q.F.; Zhou, X.H.; Zuo, J.L.; You, X.Z. Cyano-Bridged Fe<sup>III</sup><sub>2</sub>Cu<sup>II</sup><sub>3</sub> and Fe<sup>III</sup><sub>4</sub>Ni<sup>II</sup><sub>4</sub> Complexes: Syntheses, Structures, and Magnetic Properties. *Inorg. Chem.*, **2007**, *46*, 3236-3244.
- [111] Bartlett, B.M.; Harris, T.D.; DeGroot, M.W.; Long, J.R. High-Spin Ni<sub>3</sub>Fe<sub>2</sub>(CN)<sub>6</sub> and Cu<sub>3</sub>Cr<sub>2</sub>(CN)<sub>6</sub> Clusters Based on a Trigonal Bipyramidal Geometry. Z. Anorg. Allg. Chem., 2007, 633, 2380-2385
- [112] Gu, Z.G.; Yang, Q.F.; Liu, W.; Song, Y.; Li, Y.Z.; Zuo, J.L.; You, Z.-Z. Cyano-Bridged Pentanuclear Fe<sup>III</sup><sub>3</sub>M<sup>II</sup><sub>2</sub> (M = Ni, Co, Fe) Clusters: Synthesis, Structures, and Magnetic Properties. *Inorg. Chem.*, **2006**, *45*, 8895-8901.
- [113] Yang, J.Y.; Shores, M.P.; Sokol, J.J.; Long, J.R. High-Nuclearity Metal-Cyanide Clusters: Synthesis, Magnetic Properties, and Inclusion Behavior of Open-Cage Species Incorporating [(tach)M(CN)<sub>3</sub>] (M = Cr, Fe, Co) Complexes. *Inorg. Chem.*, 2003, 42, 1403-1419.
- [114] Bianchini, C.; Masi, D.; Meli, A.; Sabat, M. Reactions of Ethyl Cyanoformate with (np<sub>3</sub>)Ni, (np<sub>3</sub>)CoH [np<sub>3</sub> = N(CH<sub>2</sub>CH<sub>2</sub>PPh<sub>2</sub>)<sub>3</sub>], and (triphos)Ni [triphos = MeC(CH<sub>2</sub>PPh<sub>2</sub>)<sub>3</sub>]. Crystal Structures of the Ethoxycarbonyl Complexes [(np<sub>3</sub>)Ni(CO<sub>2</sub>Et)]BPh<sub>4</sub> and (triphos)Ni(CN)(CO<sub>2</sub>Et). *Organometallics*, **1986**, *5*, 1670-1675.
- [115] Rupp, R.; Huttner, G.; Kircher, P.; Soltek, R.; Buchner, M. Coordination Compounds of tripodCo<sup>II</sup> and tripodCo<sup>II</sup> Selective Substitution and Redox Behavior. *Eur. J. Inorg. Chem.*, **2000**, *8*, 1745-1757
- [116] Jacob, V.; Huttner, G.; Kaifer, E.; Kircher, P.; Rutsch, P. Synthesis of Oligomeric Compounds from tripodIron(II) Species Using Cyano Bridging Ligands - Electronic Coupling of Two Metal Termini Through Metal Dicyano and Diisocyano Entities. Eur. J. Inorg. Chem., 2001, 11, 2783-2795.
- [117] Contakes, S.M.; Kuhlman, M.L.; Ramesh, M.; Wilson, S.R.; Rauchfuss, T.B. Systematic assembly of the double molecular boxes: {Cs⊂[CpCo(CN)₃]₄[Cp\*Ru]₃} as a tridentate ligand. *Proc. Natl. Acad. Sci.*, **2002**, *99*, 4889-4893.
- [118] Klausmeyer, K.K.; Wilson, S.R.; Rauchfuss, T.B. Alkali Metal-Templated Assembly of Cyanometalate Boxes (NEt<sub>4</sub>)<sub>3</sub>{M-[Cp\*Rh(CN)<sub>3</sub>]<sub>4</sub>[Mo(CO)<sub>3</sub>]<sub>4</sub>} (M = K, Cs). Selective Binding of Cs<sup>+</sup>. *J. Am. Chem. Soc.*, **1999**, *121*, 2705-2711.
- [119] Contakes, S.M.; Klausmeyer, K.K.; Milberg, R.M.; Wilson, S.R.; Rauchfuss, T.B. The Seven-Component Assembly of the Bowl-

- $Shaped \quad Cages \quad Cp^*{}_{7}Rh_{7}(CN)_{12}{}^{2+} \quad and \quad Cp^*{}_{7}Rh_{3}Ir_{4}(CN)_{12}{}^{2+}. \quad \textit{Or-}$ ganometallics, 1998, 17, 3633-3635.
- [120] Contakes, S.M.; Klausmeyer, K.K.; Rauchfuss, T.B. Coordination Solids Derived from  $Cp^*M(CN)_3$  (M = Rh, Ir). *Inorg. Chem.*, **2000**,
- Kuhlman, M.L.; Rauchfuss, T.B. Structural Chemistry of "Defect" [121] Cyanometalate Boxes:  $\{Cs \subset [CpCo(CN)_3]_4[Cp^*Ru]_3\}$  and  $\{M \subset -(CpCo(CN)_3)_4[Cp^*Ru]_3\}$  $[Cp^*Rh(CN)_3]_4[Cp^*Ru]_3\}$  (M = NH<sub>4</sub>, Cs). J. Am. Chem. Soc., 2003, 125, 10084-10092
- [122] Funck, K.E.; Hilfiger, M.G.; Berlinguette, C.P.; Shatruk, M.; Wernsdorfer, W.; Dunbar, K.R. Trigonal-Bipyramidal Metal Cyanide Complexes: A Versatile Platform for the Systematic Assessment of the Magnetic Properties of Prussian Blue Materials. Inorg. Chem., 2009, 48, 3438-3452, and references cited therein.
- Li, D.; Parkin, S.; Wang, G.; Yee, G.T.; Holmes, S.M. Synthesis and Spectroscopic and Magnetic Characterization of Tris(3,5-Dimethylpyrazol-1-yl)borate Iron Tricyanide Building Blocks, a Cluster, and a One-Dimensional Chain of Squares. Inorg. Chem., 2005, 45, 1951-1959.
- [124] Wang, S.; Zuo, J.L.; Zhou, H.C.; Song, Y.; You, X.Z. Two cyanobridged heterotrinuclear complexes built from [(Tp)Fe(CN)<sub>3</sub>] (Tp = hydrotris(pyrazolyl)borate): synthesis, crystal structures and magnetic properties. Inorg. Chim. Acta., 2005, 358, 2101-2106.
- Li, D.; Parkin, S.; Wang, G.; Yee, G.T.; Clérac, R.; Wernsdorfer, W.; Holmes, S.M. An S = 6 Cyano-bridged Octanuclear  $Fe_{4}^{III}Ni_{4}^{II}$ Complex that Exhibits Slow Relaxation of the Magnetization. J. Am. Chem. Soc., 2006, 128, 4214-4215.
- Li, D.; Clérac, R.; Parkin, S.; Wang, G.; Yee, G.T.; Holmes, S.M. [126] An S = 2 Cyano-bridged Trinuclear  $Fe^{III}_2Ni^{II}$  Single-Molecule Magnet. Inorg. Chem., 2006, 45, 5251-5253.
- [127] Zhang, Y.Z.; Mallik, U. P.; Clérac, R.; Rath, N.; Holmes, S.M. Irreversible solvent-driven conversion in cyanometalate {Fe<sub>2</sub>Ni}<sub>n</sub> (n = 2, 3) single-molecule magnets. Chem. Commun., 2011, 47, 7194-7196.
- Li, D.; Clérac, R.; Parkin, S.; Wang, G.; Yee, G. T.; Holmes, S. M. [128] Ancillary Ligand Functionalization of Cyanide-bridged S = 6Fe<sup>III</sup><sub>4</sub>Ni<sup>II</sup><sub>4</sub> Complexes for Molecule-Based Electronics. *Inorg.* Chem., 2006, 45, 7569-7571.
- Liu, W.; Wang, C.F.; Li, Y.Z.; Zuo, J.L.; You, X.Z. Structural and Magnetic Studies on Cyano-Bridged Rectangular  $Fe_2M_2$  (M = Cu, Ni) Clusters. Inorg. Chem., 2006, 45, 10058-10065.
- [130] Kim, J.; Han, S.; Lim, J.M.; Choi, K.Y.; Nojiri, H.; Suh, B.J. Single molecule magnet: Heterodinuclear cyano-bridged cubic cluster  $[(Tp)_8Fe_4Ni_4(CN)_{12}]$  (Tp = hydrotris(1-pyrazolyl)borate). *Inorg*. Chim. Acta., 2007, 360, 2647-2652.
- Gu, Z.G.; Liu, W.; Yang, Q.F.; Zhou, X.H.; Zuo, J.L.; You, X.Z. Cyano-Bridged  $Fe^{III}_2Cu^{II}_3$  and  $Fe^{III}_4Ni^{II}_4$  Complexes: Syntheses, Structures, and Magnetic Properties. Inorg. Chem., 2007, 46, 3236-
- [132] Li, D.; Parkin, S.; Clerac, R.; Wang, G.; Yee, G. T.; Holmes, S. M. Structural Distortion and Magnetic Behavior in Cyanide-Bridged Fe<sup>III</sup><sub>2</sub>Ni<sup>II</sup><sub>2</sub> Single-Molecule Magnets. Eur. J. Inorg. Chem., 2007, 10, 1341-1346.
- Wang, C.F.; Liu, W.; Song, Y.; Zhou, X.H.; Zuo, J.L.; You, X.Z. [133] Syntheses, Structures, and Electrochemical and Magnetic Properties of Rectangular Heterobimetallic Clusters Based on Tricyanometallic Building Blocks. Eur. J. Inorg. Chem., 2008, 5, 717-727.
- [134] Wu, D.; Zhang, Y.; Huang, W.; Sato, O. An S = 3 cyanide-bridged tetranuclear  $Fe^{III}_2Ni^{II}_2$  square that exhibits slow relaxation of magnetization: synthesis, structure and magnetic properties. Dalton Trans., 2010, 39, 5500-5503.
- [135] Zhang, Y.Z.; Mallik, U.P.; Rath, N.; Yee, G.T.; Clérac, R.; Holmes, S.M. A cyano-based octanuclear {Fe<sup>III</sup><sub>4</sub>Ni<sup>II</sup><sub>4</sub>} single-molecule magnet. Chem. Commun., 2010, 46, 4953-4955.
- Peng, Y.H.; Meng, Y.F.; Hu, L.; Li, Q.X.; Li, Y.Z.; Zuo, J.L.; You, X.Z. Syntheses, Structures, and Magnetic Properties of Heterobimetallic Clusters with Tricyanometalate and  $\pi$ -Conjugated Ligands Containing 1,3-Dithiol-2-ylidene. Inorg. Chem., 2010, 49, 1905-1912.

- Hoshino, N.; Sekine, Y.; Nihei, M.; Oshio, H. A chiral single mole-[137] cule magnet and chiral single chain magnet. Chem. Commun., **2010**, 46, 6117-6119.
- [138] Nihei, M.; Okamoto, Y.; Sekine, Y.; Hoshino, N.; Shiga, T.; Liu, I.P-C.; Oshio, H. A Light-Induced Phase Exhibiting Slow Magnetic Relaxation in a Cyanide-Bridged [Fe<sub>4</sub>Co<sub>2</sub>] Complex. Angew, Chem., Int. Ed., 2012, 51, 6361-6364.
- [139] Zhang, Y.Z.; Mallik, U.P.; Rath, N.P.; Clérac, R.; Holmes, S.M. Pyrazolylborates and Their Importance in Tuning Single-Molecule Magnet Properties of {Fe<sup>III</sup><sub>2</sub>Ni<sup>II</sup>} Complexes. *Inorg. Chem.*, **2011**, 50, 10537-10539.
- [140] Zhang, Y.Z.; Li, D.F.; Clérac, R.; Holmes, S.M. A cyanide-bridged trinuclear {Fe<sup>III</sup><sub>2</sub>Ni<sup>II</sup>} complex decorated with organic radicals. Polyhedron, 2013, 60, 110-115.
- Zhang, Y.Z.; Mallik, U.P.; Clérac, R.; Rath, N.P.; Holmes, S.M. Structure-property trends in cyanido-bridged tetranuclear Fe<sup>III</sup>/Ni<sup>II</sup> single-molecule magnets. Polyhedron, 2013, 55, 115-121.
- Beedle, C.C.; Zhang, Y.Z.; Holmes, S.M.; Hill, S. EPR studies of a [142] cyanide-bridged {Fe<sup>III</sup><sub>2</sub>Ni<sup>II</sup>} coordination complex and its corresponding Fe<sup>III</sup> mononuclear building block. *Polyhedron*, **2013**, *50*, 48-51.
- Zhang, Y.-Z.; Clérac, R.; Holmes, S.M. A magnetic cyanidebridged {Fe<sup>III</sup><sub>2</sub>Ni<sup>II</sup>} complex and its tricyanoferrate(III) building block. Submitted for publication.
- [144] Cho, K.J.; Ryu, D.W.; Kwak, H.Y.; Lee, J.W.; Lee, W.R.; and Lim, K.S.; Koh, E.K.; Kwon, Y.W.; and Hong, C.S. Designed cyanide-and phenoxide-bridged Fe<sup>III</sup>Mn<sup>III</sup> single-molecule magnet constructed by highly blocked paramagnetic precursors. Chem. Commun., 2012, 48, 7404-7406.
- [145] Cho, K.J.; Ryu, D.W.; Lim, K.S.; Lee, W.R.; Lee, J.W.; Koh, E.K.; Hong, C.S. Syntheses, structures, and magnetic properties of cyano- and phenoxide-bridged Fe(III)-Mn(III) tetrameric assemblies formed by blocked fac-Fe tricyanide with aliphatic rings. Dalton Trans., 2013, 42, 5796-5804.
- Jurca, T.; Farghal, A.; Lin, P.H.; Korobkov, I.; Murugesu, M.; [146] Richeson, D.S. Single-Molecule Magnetic Behavior with a Single Metal Center Enhanced through Peripheral Ligand Modification. J. Am. Chem. Soc., 2011, 133, 15814-15817.
- [147] Kim, J.; Han, S.; Cho, I.K.; Choi, K.Y.; Heu, M.; Yoon, S.; Suh, B. J. Synthesis of a cyano-bridged Fe<sub>2</sub>Mn linear unit and a Fe<sub>2</sub>Mn<sub>2</sub> square by using the [fac-Fe{HB(pz)<sub>3</sub>}(CN)<sub>3</sub>] building block. Polyhedron, 2004, 23, 1333-1339.
- [148] Harris, T.D.; Long, J.R. Linkage isomerism in a face-centers cubic  $Cu_6Cr_8(CN)_{24}$  cluster with an S=15 ground state. Chem. Commun., **2007**, (13), 1360-1362.
- [149] Wang, S.; Zuo, J.L.; Zhou, H.C.; Song, Y.; Gao, S.; You, X.Z. Heterobimetallic Complexes Based on [(Tp)Fe(CN)3]: Syntheses, Crystal Structures and Magnetic Properties. Eur. J. Inorg. Chem., 2004, 18, 3681-3687.
- Yao, M.X.; Wei, Z.Y.; Gu, Z.G.; Zheng, Q.; Xu, Y.; Zuo, J.L. Syntheses, Structures, and Magnetic Properties of Low-Dimensional Heterometallic Complexes Based on the Versatile Building Block [(Tp)Cr(CN)<sub>3</sub>]. Inorg. Chem., 2011, 50, 8636-
- Kim, J.; Han, S.; Pokhodnya, K.I.; Migliori, J.M.; Miller, J.S. [151] Cyano-Bridged Hexanuclear Fe<sub>4</sub>M<sub>2</sub> (M = Ni, Co, Mn) Clusters: Spin-Canted Antiferromagnetic Ordering of Fe<sub>4</sub>Ni<sub>2</sub> Cluster. Inorg. Chem., 2005, 44, 6983-6988.
- [152] Wang, X.Y.; Avendaño, C.; Dunbar, K.R. Molecular magnetic materials based on 4d and 5d transition metals. Chem. Soc. Rev., **2011**, 40, 3213-3238.
- [153] Palii, A.; Tsukerblat, B.; Klokishner, S.; Dunbar, K.R.; Clemente-Juan, J.M.; Coronado, E. Beyond the spin model: exchange coupling in molecular magnets with unquenched orbital angular momenta. Chem. Rev. Soc., 2011, 40, 3130-3156.
- Freedman, D.E.; Jenkins, D.M.; Iavarone, A.T.; Long, J.R. A Redox-Switchable Single-Molecule Magnet Incorporating [Re(CN)<sub>7</sub>]<sup>3</sup>. J. Am. Chem. Soc., 2008, 130, 2884-2885.
- [155] Bennett, M.V.; Long, J.R. New Cyanometalate Building Units: Synthesis and Characterization of  $[Re(CN)_7]^{3-}$  and  $[Re(CN)_8]^{3-}$  J. Am. Chem. Soc., 2003, 125, 2394-2395.